KTH Industrial Engineering
and Management

Numerical Modelling and Experimental Validation of Heat Pipe Solar Collector for Water Heating

By Abebe Kebede Endalew

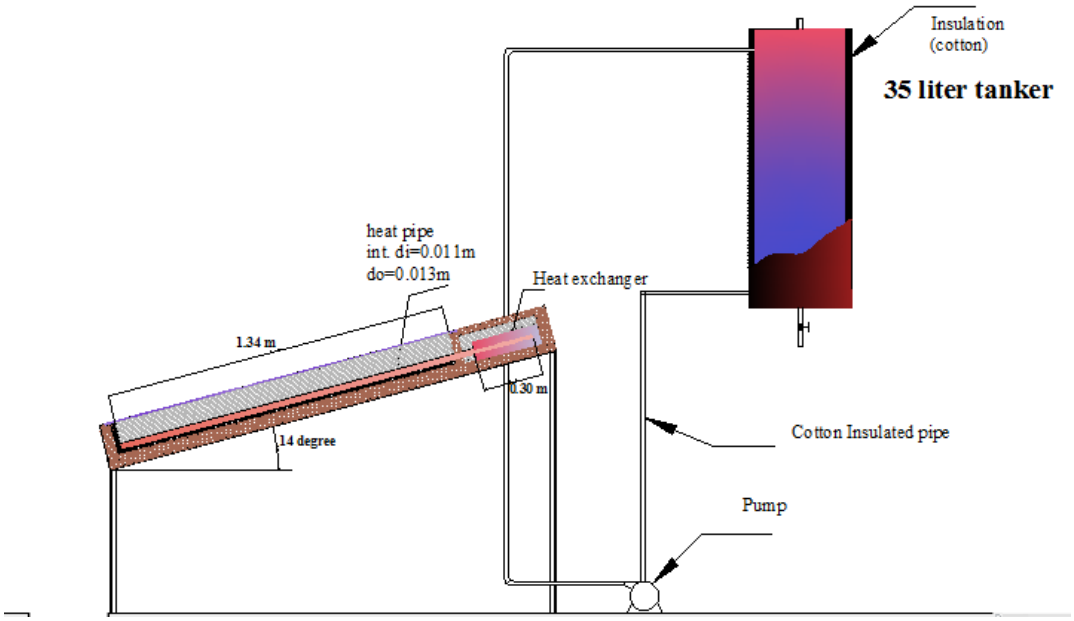

Master of Science Thesis

KTH School of Industrial Engineering and Management
Energy Technology EGI-2011-128MSc
Division of Applied Thermodynamic and Refrigeration
SE-100 44 Stockholm , Sweden

Master of Science Thesis EGI-2011-128MSC

KTH Industrial Engineering and Management

Numerical Modeling and Experimental Validation of Heat Pipe Solar Collector for Water Heating

Abebe Kebede Endalew

Approved Date February 3, 2012 Stockholm, Sweden	Examiner: Professor Björn Palm KTH -School of Industrial Engineering and Management, Energy Technology, Division of Thermodynamics and Refrigeration	Supervisors: Professor Björn Palm KTH -School of Industrial Engineering and Management, Energy Technology, Division of Thermodynamics and Refrigeration Dr. Solomon Teferi Bahir Dar University, Department of Mechanical Engineering, Bahir Dar , Ethiopia
	Commissioner	Contact person

Abstract

This work studies the performance of heat pipe solar collector for water heating. Experimental results are validated using numerical modeling. Homemade heat pipes with distilled water as a working fluid were used for experimental tests. Both natural and forced convective heat pipe condensing mechanisms are studied and their results are compared with conventional natural circulation solar water heating system. Cross flow and parallel flow heat exchanger were tested in forced type heat pipe condensing mechanism. Experimental and numerical results showed good agreement. Heat pipe solar collectors outperformed conventional solar collector because of their efficient heat transport method. Forced convective heat exchanger was found to give higher efficiency compared to natural convective heat pipe condensing system. However, natural convective heat pipe condensing is free from parasitic power and low system weight. It also showed appreciable system efficiency and can be further developed to be used in rural areas where grid electricity is scarce. Cross flow and parallel flow heat exchanger have been tested for forced convective heat pipe condensing mechanism and no appreciable difference was found due to higher fluid velocity in heat exchangers.

Acknowledgment

I sincerely thank Stiftelsen Futura for the fund to follow this fascinating program. Without this support it could have been impossible. I also thank the Department of Energy Technology (KTH) for creating this interesting program through distance based and their patience for during the course of study. The Ethiopian Science and Technology Commission is also acknowledged for funding this thesis work through the research fund "Solar Water Heater Employing Heat Pipes" with research number FST/023/2005-Mekelle University.

My sincere thank goes to my thesis supervisor Professor Björn Palm from KTH who provided me valuable comments and his patience for the long waited thesis work. I also thank my local supervisor Dr. Solomon Teferi from Bahir Dar University for his help during my thesis work. I should also thank Mr. Micheal G/Yesus and Dr. Mulu Bayray from Mekelle University for their technical help during system manufacturing and testing.

Abebe K. Endalew

Bahir Dar, December, 2011

Table of Contents

List of Figures

List of Tables

Nomenclature

Q-	Heat transfer [W]
H-	Heat of evaporation [KJ/Kg]
L,l	Length [m]
P-	Pressure [N/m^2]
R	Universal gas constant
T	Temperature [^{o}C] or [K]
k	Thermal conductivity [w/m^2.k]
K_p	Wick permeability [m^2]
A	Area [m^2]
r	Radius [m]
h	Convective Heat transfer coefficient [W/m2.K]
g	Gravitational acceleration [m/s^2]
G_{on}	extraterrestrial radiation[W/m^2]
G_{sc}	Solar constant [W/m^2]
I	Total solar radiation on ground [W/m^2]
K_T	clearance index
S	Absorbed solar radiation [W/m^2]
T_{hf}	Temperature of heat pipe working fluid [^{o}C]
T_w	Tanker water temperature [^{o}C]
T_a	Ambient temperature [^{o}C]
h_r	Radiative heat transfer coefficient [W/m2.K]
T_b	Tube base temperature [^{o}C]
Q_u	Absorbed heat [w]
q	Heat per unit area [W/m^2]
T_s	Sky temperature [^{o}C]
Nu	Nusselt number
Ra	Rayleigh number
Pr	Prandtle number
Re	Reynolds number
u	Fluid velocity
U_t	Collector top Heat transfer coefficient [W/m2.K]
R	Heat transfer resistance [m^2.K/W]
Z,z	Height [m]
Greek letter	
ϱ	Density [kg/m^3], solar reflectance
σ_s	Surface tension
μ	Dynamic viscosity
β	Collector inclination angle [^{o}]
γ	Specific heat ratio
θ	incident angle with the tilted surface
ϱ_g	Ground reflectance
θ_z	zenith angle
ϕ	Latitude
γ_z	surface azimuth angle
ε	Emissivity
ϱ_r	Reflectance
a	Absorptance
(τa)	Transmittance-absorptance product
σ	Boltzmann constant
β'	Volumetric coefficient of expansion
ν	Kinematic viscosity
a_d	Thermal diffusivity
δ	Plate thickness [m]
η	Efficiency
Subscripts	
p	Plate , pumping pressure
v	Vapor
l	Liquid
e, eff	Effective

U_L	Total heat transfer coefficient [W/m2.K]	*t*	Total
U_b	Collector bottom heat transfer [W/m2.K]coefficient	*w*	Wick, water
Upip	Water tube heat transfer coefficient [W/m2.K]	*h*	Hydraulic diameter
U_{tank}	Water tank heat transfer coefficient [W/m2.K]	*o*	Initial ,external
U_e	Edge heat transfer coefficient [W/m2.K]	*i*	Internal
W	Absorber plate width [m]	*cond*	Heat pipe condenser
D, d	Diameter [m]	*hp*	Heat pipe
x	Distance [m]	*evap*	Evaporator
F	Fin efficiency	*b*	beam
C_b	Bond conductance [W/m2.K]	*d*	Diffuse
F'	Collector efficiency factor	*cs*	circumsolar
T_f	Fluid temperature [^{o}C]	*refl*	Reflected
F_R	Heat removal factor	*hr*	Horizon
F"	Flow factor	*c-a*	Cover –ambient
C	Capacitance [KJ/Kg. K]	*p-c*	Plate –cover
c	Specific capacitance [KJ/K]	*b-a*	Bottom –ambient
f	Friction factor	*c-s*	Cover to sky
$\dot{m}$	Mass flow [kg/s]	*exh*	Heat exchanger
P	Pressure [N/m^2]	*tan*	tank
P_{fr}	Friction head [m]	*pip*	Pipe
P_ϱ	Thermal pressure head [m]	*m*	Fluid Mean value

1. Introduction

The demand for energy is increasing at a substantial rate as the economy of the populous developing countries is growing. Currently, this high energy demand mainly depends on fossil fuel resources. Apart from the difficulty of meeting the high energy demand, the issue of environment and sustainability has led to a critical concern on power generation and its utilization. Fossil fuels are sources of emissions and are unsustainable due to their dwindling reserves, price rise and resource not evenly distributed in the world. Geopolitical instability in resource areas is also a major concern. Following this, today's agenda is power production from renewable resources which are environmentally benign and sustainable. Renewable energy sources such as solar energy are the long term options to substitute conventional energy systems.

Substantial amount of heat energy is used for space heating and hot water production in household energy system depending on the geographical location. In the Sweden for instance, space heating and domestic hot water accounts approximately 60% of the residential energy use in 2009 (Swedish Energy Agency, 2010) while it accounts 19.2% of the household energy demand in US in 2001 (US Department of energy, 2005) and 81.1% of the household energy in Canada in 2002 (Aguilar et al., 2005). The use of renewable energy technologies for production of heat energy can play a significant role in reducing the demand of fossil fuels for heat energy production and reduce CO_2 emission.

Solar water heaters are the most developed renewable energy technologies used in the world. For the past several years, conventional flat plate collectors have been well studied and developed. Their relatively low cost, lower maintenance and easy of construction have made these systems very competitive and are widely used all over the world specially for low temperature thermal systems. Conventional flat plate solar collectors use water pipes attached to the collecting where water circulates either naturally or forced inside the pipes and so transfers the heat collected by the plate to the storage tank. The following are some of the limitations of conventional flat plate solar collectors for water heating (Kreider and Kreith, 1997; Francis de Winter, 1990; Duffie and Beckman, 1991).

- Low heat transported by the fluid which leads to low thermal efficiency
- Pipe corrosion due to the use of water
- Freezing of water used in cold nights
- The night-cooling effect due to the transverse flow of cooled water
- The extra space required for natural circulation due to the position limitation required
- And the heavy total system weight

A design improvement of conventional flat plate collectors increases the solar energy share for hot water production. Due to the low energy density and transient nature of solar energy, designing appropriate heat transport system is important in increasing the solar fraction for stand alone or simulated hot water production systems.

Employing heat pipes for solar water heating application is at its young stage and extensive studies are required to integrate heat pipe in solar collector systems so as to improve the heat transport. Since the advent of heat pipes in 1960, their importance in solar application such as solar collectors for domestic water heating, space heating and cooling has received increasing attention (Dunn and Reay, 1994). As the demand of energy conservation increases, heat pipes become more and more attractive for an increasing number of various applications. Heat pips have low thermal resistance for heat transfer than any other metals have (Dunn and Reay, 1994). Most of the above limitations of conventional solar collectors can be overcome by using a compact heat pipe solar collector system. Very high thermal conductance (phase change heat transfer), the ability to act as a thermal flux transformer and an isothermal surface of low thermal impedance are very important properties of heat pipe for solar system application.

Several studies have been reported on the use of heat pipe for solar water heating systems. Ismail and Abogderah (1998) presented both theoretical and experimental comparison of wicked heat pipe solar collector and compared with conventional forced solar collector. Methanol was used for heat pipe working fluid and the condenser was 15 degree more inclination than the collector for better condensate return. The theoretical study was based on Duffie and Beckham (1991). Heat pipe solar collector was found with high efficiency compared to the conventional solar collector. Theoretical and experimental studies on wickless heat pipe solar collectors for water heating have been reported (Hussein, 1999, 2007). These studies use cross flow condenser heat exchanger. Distilled water was used as working fluid in heat pipes. The performance of wickless heat pipe solar collector was found to be sensitive to cooling water inlet temperature, absorber plate material and thickness and condenser length. It was also possible to know the optimum cooling water mass flow rate for best efficiency of the system. The effect of condenser heat transfer on the performance of plate type heat pipe solar collector with cross flow condenser heat exchanger was studied using CFD methods (Facao and Oliveira, 2005). Due to non-uniform velocity pattern in the heat exchanger, a mixed of natural and forced convective heat transfer models was considered and found to have better match with experimental results. However, there is scarce of study on the effect of different types of heat pipe condensers on the system performance of heat pipe solar collectors. In this study, both forced and natural convective heat transfer in condenser heat exchanger are studied and their performance is compared for the first time. The performance of natural convective heat pipe condenser type is compared with conventional natural circulation solar water heating system.

2. Objective of the Project

The objective of this thesis is to study the integration of heat pipe for flat plate solar collector for water heating. The project aims to evaluate the performance of heat pipe solar water heaters with conventional flat plate solar water heating system. The project also investigates the effect of heat pipe condensing types on the performance of the system.

Related scientific works are reviewed and documented. Single-node flat plate solar collector model has been adapted for collector modeling from Duffie and Beckham (1991) and transient system heat transfer equations are developed and solved numerically using Matlab. A homemade heat pipe and collector systems are used for the experimental validation. All manufacturing and system testing are done at Mekelle University, Department of mechanical Engineering. Both numerical and experimental results will be compared and interpreted accordingly.

3. Working Principle of Heat Pipe

The components of a typical cylindrical wicked heat pipe are copper tube with end sealed, wick structure, and a small amount of working fluid in thermal equilibrium with its vapor. It has three main sections as shown in Figure 1: the evaporator, adiabatic and the condenser sections. In solar collectors, the evaporator is bonded with the absorber of the collector and the condenser section is inserted in to the heat exchanger. The heat picked by the evaporator sinks at the condenser section. Heat loss in the adiabatic section is mostly ignored for good insulation. The working fluid is maintained at lower pressure in the heat pipe. The working fluid evaporates at the evaporator section and creates a vapor pressure to flow to the condenser section to condense. The evaporation and condensation happens at saturated temperature. The wick develops a capillary pressure to pump condensed liquid from condenser to evaporator to complete the circulation. The pumping can also be done by gravitation in gravity assisted heat pipes which is also common in solar collectors.

3.1. Heat Pipe Theory and Design

In the design of heat pipe, the characteristic of the three main components: the working fluid, the wick and the container are of important to attain the required heat transport capacity.

In order the heat pipe to work, the pressure drop in the fluid flow has to be compensated by the pumping pressure in the wick by capillarity (Dunn and Reay, 1994). In equation form

$$\Delta P_p = \Delta P_l + \Delta P_v + \Delta P_g \qquad (1)$$

Where ΔP_p, ΔP_l, ΔP_v and ΔP_g are the total pumping pressure, pressure drop for liquid return from condenser, pressure drop for vapor flow in the evaporator and gravity head, respectively.

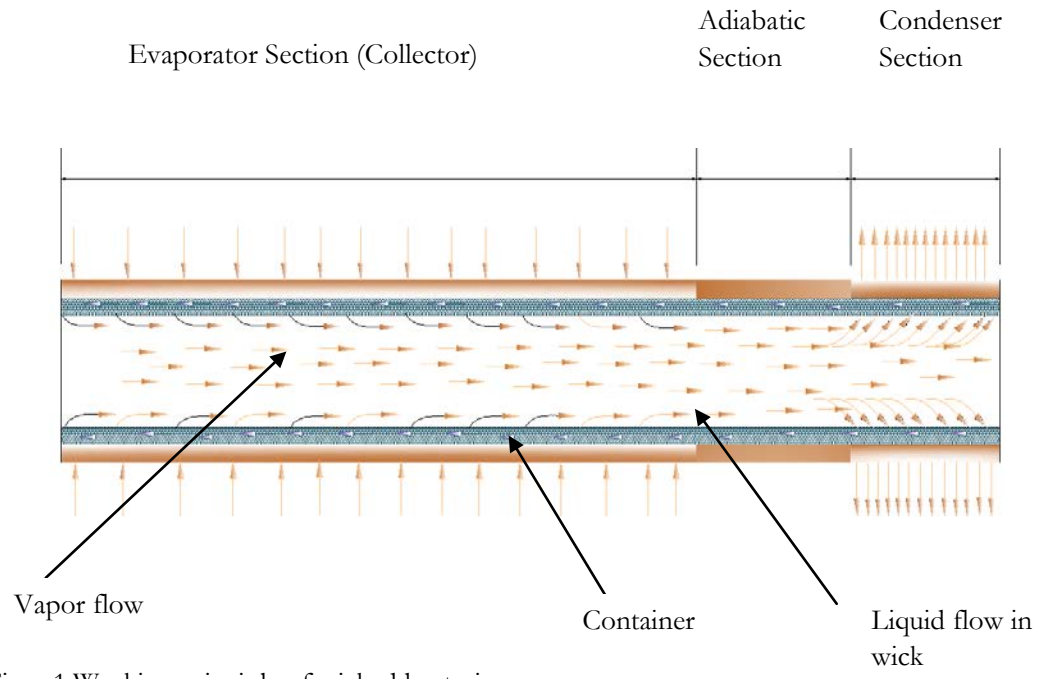

Figur 1.Working principle of wicked heat pipe

3.2. Heat Transfer Limits

The physical properties of the fluid used and the wick properties determine the design to achieve a working heat pipe with required heat flux. Capillary, sonic, entrainment, boiling, frozen start up, continuum vapor, vapor pressure and condenser effects are physical phenomena that limit heat pipe heat transfer. The heat transfer limit for heat pipe can be caused by any of the above phenomena depending on the construction of the heat pipe and the operating environment. The lowest limit of these phenomena is considered as a design limit. The main design limitations are discussed as follows (Dunn and Reay (1994); Faghri (1995); Reay and Kew (2006)).

Capillary limit (Wicking limit):

The circulation of working fluid between the end zones happens due to the presence of wick structure. This limitation is very common in low temperature heat pipes for instance in hot water production. The limitation occurs when the capillary pumping power is not enough to overcome the pressure drops. The evaporator dries out if heat transfer above this capillary limit is attempted. The maximum heat transfer (Q_{max}) calculation is based on the hydrodynamic properties of the working fluid, wick and the orientation of heat pipe.

$$Q_{\max} = \left[\frac{\rho_l \sigma_l H}{\mu_l}\right]\left[\frac{K_p A_w}{l_e}\right]\left[\frac{2}{r_e} + \frac{\rho_l g l_t \sin\beta}{\sigma_l}\right] \tag{2}$$

Where ϱ, σ, μ are the density, capillarity and viscosity of the liquid fluid; K - permeability of the wick, A_w - wick area, θ-inclination of heat pipe from horizontal, r_e-effective radius of the heat pipe, g- gravitational acceleration, *l*- total length of the heat pipe, H- heat of evaporation of the working fluid, subscript *l*- liquid.

Sonic Limit

Heat pipe operation is accompanied with extraction and addition of mass in the evaporator and condenser. The vapor velocity increases along the evaporator and reaches maximum at the end of the evaporator. Since the vapor diameter is constant the heat pipe can act a nozzle at the end of the evaporator. Since the vapor velocity cannot be greater than the speed of sound, a sonic limit develops.

$$Q_{\max} = A_v \rho_v H\left[\frac{\gamma_v R_v T_v}{2(\gamma_v + 1)}\right]^{0.5} \tag{3}$$

Where γ_v is the vapor specific heat ratio, R_V- gas constant, and T_v - temperature

Entrainment limit

This limitation happens when water droplets are transported by the fast moving vapor due the shear force between the vapor and liquid at the interphase. If the heat transfer is too high, the evaporator dries out and the heat pipe stops working. Therefore, the maximum heat transfer possible with this limit is

$$Q_{\max} = A_v H\left[\frac{\sigma_{s,l}\rho_v}{2r_h}\right]^{0.5} \tag{4}$$

Where r_h is hydraulic radius of porous media.

Boiling limit

Heat pipe wall temperature in the evaporator can become too high when the liquid in the wick starts to boil due to high radial heat flux. The vapor bubbles in the wick prevent the liquid for uniform wetting and a hot spot produces. This leads a dry out in the evaporator and limits the heat transfer.

$$Q_{\max} = \frac{2\pi l_e k_e T_v}{H\rho_v \ln\left(\frac{r_i}{r_v}\right)}\left[\frac{2\sigma_{s1}}{r_o} - P_o\right] \tag{5}$$

Where l_e -evaporator length, k_e - conductivity of the wick material, P_0- working pressure, subscript i,v, and 0 are internal , vapor and external respectively.

3.3. Selection of Heat Pipes

Heat pipe are classified based on construction and operation. Two-phase closed thermosyphon wickless gravity assisted and capillary driven are the most common heat pipe types used in solar application. Gravity is the main mechanism in the thermosyphon type to return the condensate from the condenser which is located above the evaporator. The entrainment limit is more profound in gravity assisted than capillary driven due to the free liquid surface. The opposite of entrainment, flooding is also a problem in thermosyphon heat pipe. Filling ratio is also very important factor in thermosyphon than capillary driven heat pipe. Dry out occurs because of pool type and non-distributed working fluid. Gravity assisted wickless are difficult in solar collectors with high degree of inclination because of pooling which create non-uniform liquid distribution along the absorber length. This creates an increase wall temperature in some part of the heat pipe.

In a capillary driven heat pipe, a wick placed circumferentially in the internal of the sealed container is used to pump the working fluid from the condenser to the evaporator. Appropriate amount of working fluid is put inside the container to saturate the wick. It has better performance in transferring heat with a small temperature drop and long distance. The capillary limit is the main heat transfer limit in capillary driven heat pipe. A combination of wicked and gravity assisted heat pipe gives a compromised performance specially for solar application where the evaporator is long compared to other sections and need a uniform wetting properties. A design of gravity assisted wicked heat pipe for solar application is presented in this work.

3.4. Working Fluid

The design of heat pipe starts with the selection of working fluid. The selection of working fluid considers a number of factors. The working temperature range is the first criteria to be fulfilled by the working fluid. In solar collector, this is a crucial step as it determines the minimum and the maximum temperature for the heat pipe operation. The following are other main criteria for selecting the right working fluid (Dunn (1994)).

- Compatibility with the wick and the container
- Good thermal stability
- Wettability of wick and wall materials
- Vapor pressure not too high or low over operating temperature
- High latent heat
- High thermal conductivity
- Low liquid and vapor viscosities
- Higher surface tension

- Acceptable freezing or pour point

Organic solvents are the most widely used working fluid for low temperature applications because of lower vapor pressure, less susceptible for freezing and material compatibility. For example Ethanol has been used in many works for solar applications (e.g. Azad, 2008; Mathioulakis. and Belessiotis, 2002; Chun et al., 1999; Payakaruk et al., 2000). But their advantage is degraded by low heat transport capacity. In solar application, the efficiency of heat transport capacity overcomes other selection criteria as for the working fluid. Hence, the use of working fluid with higher latent heat is beneficial. Water gives superior property most of the organic solvents. Water is compatible with copper which is the most common container and wick material used today. Water is considered for heat pipe working fluid in this work.

3.5. Container and Wick

The purpose of the container is to isolate the working fluid and the wick from external environment and keep the required working pressure. It has to maintain the pressure differentials during operation of the heat pipe. Thermal conductivity, strength to weight ratio and simplicity of fabrication method are important factors in the selection of material for container. Wettability and porosity are also important factors for uniform fluid distribution. Copper has surpassed properties for these properties and it is used in this work.

Many factors decide the selection of wick materials and its structure. The property of the working fluid is one of the important factors to be considered. Since its ultimate goal is to create a pumping pressure from condenser to the evaporator, the wick has to produce the required capillary. Permeability is also a desirable property to be considered in wick design. Both depend on the pore size of the wick. Capillary action increase with decreases the pore size and the reverse happens for the permeability. The wick should have also a good thermal conductivity for minimum heat resistance. There are different types of wick designs. The two most common types are homogeneous structure and arterial wicks.

Homogeneous structures can be in mesh or twills. These are simplest and the common type wicks used. It can be produced from stainless steel, copper, aluminum and nickel. A copper mesh type wick is used in this experimental work.

3.6. Dimensioning Heat Pipe Section

The heat collected at the evaporator (solar absorber) has to be dissipated in the condenser. This needs a careful design of evaporator and condenser length. The condenser length depends on the amount of heat collected and the condensation mechanisms. High heat transfer coefficient in condenser heat exchanger results small condenser length. This can be attained by increasing the velocity of the condensing fluid or

any other mechanisms which can increase the heat transfer. The size of the evaporator and the cooling fluid temperature also determine the condenser length. Critical design values have to be considered in sizing the sections of the heat pipe. The adiabatic section depends on how long should be the heat transferred from the evaporator. In solar water heaters the length of adiabatic section doesn't have a merit mostly. Therefore, it is desirable to reduce the adiabatic length as small as possible to minimize the heat loss. For the heat collected from the solar absorber, the condenser length can be optimized:

$$\frac{\dot{Q}_{collector}}{h(T_{hf} - T_w)} = \pi d_{o,hp} l_{cond} \tag{6}$$

4. Flat plate Solar Collectors

In fluid heating, flat plate solar collectors are the most developed and adapted solar technologies for low and medium temperature thermal applications. Solar radiation heats absorber and a heat transfer fluid transports heat from the absorber. Flat plate solar collectors are inexpensive, robust, and developed construction and have got wide applications in solar technologies. A typical single glazed flat plate solar collector is shown in Figure 1. The special optical characteristic of flat plate collector is its advantage in using both beam and diffuse solar radiation. For residential and commercial use, flat plate collectors can produce heat sufficiently high temperature to heat swimming pools, domestic hot water, and buildings. Temperatures of 40 to 70 ^{0}C can easily be attained by flat plate collectors (Duffie & Beckman, 1991). Careful engineering design of materials and heat transfer system can improve the efficiency of solar collecting. Conventional flat plate collectors have the following basic components:

- A transparent cover of one or more layers of glass or plastic material that transmits visible and near infrared radiation wavelength (<3 μm) and absorbs far infrared radiation wavelength (> 3 μm). In flat plate collectors, the cover has three main advantages. The first is to return the reflected beam of the solar radiation from the absorber and increase the absorptance of the absorber. The second advantage of the cover is that it traps the thermal radiation emitted from the black absorber which decease the thermal loss from the collector systems. The third and the last is to isolate the hot black absorber from the ambient condition so that it decreases the heat loss.
- An absorber plate made of a high thermal conductive material, coated with a selective material having a high solar absorptance and a low thermal emissivity (Duffie & Beckman, 1991).
- Metal tubing or channels through which the heat transfer fluid passes and which are likely to be coated with the same material as the absorber plate.
- A casing or container encasing these components, with insulating material on the back of the absorber plate or casing, and on the casing sides to minimize heat losses.

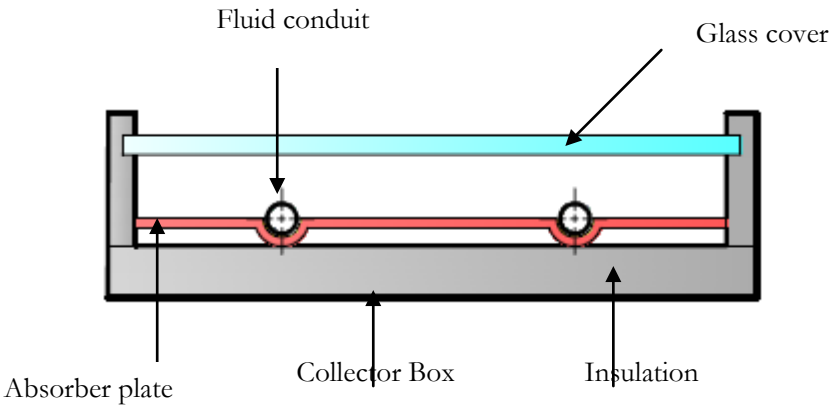

Figur 2. Single-Cover typical flat plate solar collector

4.1. Solar Radiation for Flat Plate Collector

Thermal radiation has a wavelength between 0.2-1000 μm in the spectrum of electromagnetic radiation. This includes all the solar radiation, infrared radiation and some of ultraviolet radiation. Solar radiation covers a wave length from visible to infrared (i.e. 0.3 to 25 μm). The study of solar energy for a specific thermal application starts from the maximum extraterrestrial energy flux of the sun, the solar constant G_{SC}. It is the energy from the sun, per unit of time, received on a unite area of surface perpendicular to the direction of propagation of the radiation, at mean earth-sun distance, outside the atmosphere. A different value of G_{SC} has been given by different reports depending on the type of measurements used. The World Radiation Center has adopted the most recent value of G_{SC} =1367 W/m² with uncertainty of order of 1%. However, the variation of the sun to earth distance leads a variation of extraterrestrial radiation flux in the range of $\pm$3%. To account this, the following equation is used to calculate the extraterrestrial radiation received (Duffie & Beckman, 1991):

$$G_{on} = G_{sc}\left(1 + 0.033\cos\frac{360n}{365}\right) \qquad (7)$$

Where, G_{on} is the extraterrestrial radiation measured on the plane normal to the radiation and on the n^{th} day of the year (with January 1 as one).

The total solar radiation reached on the surface is subjected to scattering and absorption of radiation in the atmosphere. Atmospheric scattering is mainly due the air molecules, water and dust while absorption is due to O_3, H_2O, and CO_2. The x-ray and other very short wave radiation of the solar spectrum are absorbed high in the ionosphere by nitrogen, oxygen and other atmospheric components. The ozone layer absorbs most of the ultraviolet. Very little part of radiation of wavelength longer than 2.5 μm reaches the earth due the high absorption by CO_2. Thus, from the viewpoint of terrestrial application of solar energy,

only radiations between 0.29 and 2.5 μm need to be considered. The solar energy reached in the earth's surface is a combination of beam and diffuse components. The diffuse component is the result of atmospheric scattering and ground reflections.

Flat plate collectors absorb both diffuse and beam radiations. Climatic conditions greatly affect the diffuse component. The first is isotropic which is received uniformly from the sky dome and the second is circumsolar diffuse resulting from forward scattering of solar radiation and concentrated in the part of the sky around the sun. The third type is the horizon diffuse type, referred as horizon brightening, is concentrated near the horizon. Figure 2 demonstrates these radiations on tilted surface. The total radiation I on the inclined surface is the sum of beam and the diffuse:

$$I = I_b + I_{d,iso} + I_{d,cs} + I_{d,hz} + I_{refl} \tag{8}$$

Where the subscripts b, d iso, cs,hz and refl refers beam ,diffuse, the isotropic, circumsolar, horizon, and reflection radiation respectively.

Duffie & Beckman (1991) has reviewed different models developed by different researches and suggested the HDKR model. HDKR refers to the integration of Hay & Davis (1980), Klucher (1979), Reindl et.al (1990a) model. The model considers the beam radiation, all components of diffuse radiation, and the ground reflection to find the total radiation on the tilted surface.

$$I = \left(I_b + I_d A_i\right)\frac{\cos\theta}{\cos\theta_z} + I_d\left(1 - A_i\right)\left(\frac{1+\cos\beta}{2}\right)\left[1 + f\sin^3\left(\frac{\beta}{2}\right)\right] + I\rho_g\left(\frac{1-\cos\beta}{2}\right) \tag{9}$$

Where , A_i is the anisotropic index which is a function of the transmittance of the atmosphere for beam radiation

$$A_i = \frac{I_b}{I_o}$$

β - tilt angle for the collector from the horizontal

θ - incident angle with the tilted surface

θ_z -zenith angle, the angle incidence of the beam radiation on the horizontal surface

ρ_g- surrounding diffuse reflectance (0.2 for non-snow surfaces)

$$f = \sqrt{\left(I_b / I\right)}$$

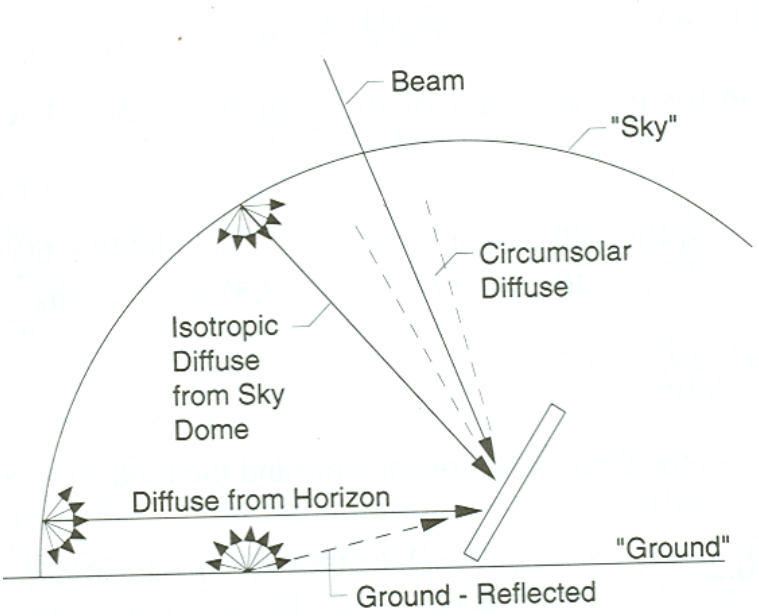

Figur 3 Beam, diffuse and ground reflected radiation on tilted surface (source: Duffie & Beckman, 1991)

4.1.1. Collector Orientation

The variation of slope and solar azimuth angle (γ) affect the amount of total energy collected in the flat plate collector during monthly, seasonally or annually. Proper optimization of these variables is important in the demand of hot water for household or industrial purpose. The surface orientation leading to maximum output of a solar energy system may be quite different from the orientation leading to maximum incident energy. Figure 3 shows the energy collected per year at different collector tilt angle β with other parameters kept constant. The total annual energy received as a function of slope is maximum at approximately $\beta = \phi$ where ϕ is the latitude. The orientation of a flat plate solar collector can also be adjusted depending on the required seasonal or monthly demand. In general, the following rule of thumb can be considered in the design of flat plate solar collector For maximum annual energy availability, a collector tilt angle equal to the latitude is considered (Duffie. & Beckman, 1991).

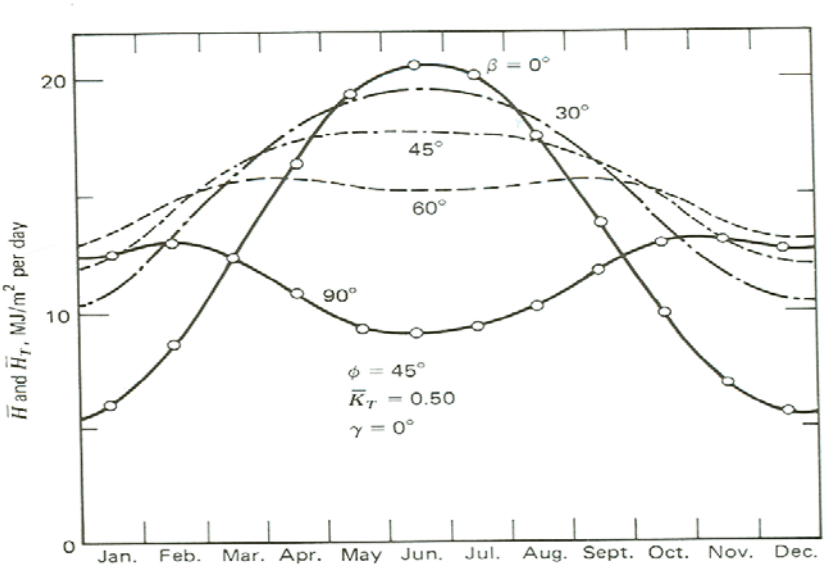

Figur 4. Variation of average daily radiation (H) on surfaces with different slope as a function of time in the year for latitude, ϕ= 45^0, average clearance index K_T =0.5 and surface azimuth angle γ=0^0, and ground reflectance ϱg=0.2.(Source: Duffie & Beckman, 1991)

4.1.2. The Relationship of Absorptivity Emissivity and Reflectivity

Radiation and optical properties of opaque and transparent materials play a significant role in the design of flat plate solar collectors. The absorptivity, emissivity and the reflectivity are the three properties of the surface or incidence radiation used in the design of a solar collector. The absorptivity (α), emissivity (ε) and reflectivity (ϱ_r) of a surface or incident radiation can be calculated as follows (Duffie & Beckman, 1991):

$$\left.\begin{aligned} \alpha &= \frac{\int_0^\infty \alpha_\lambda G_{\lambda,i} d\lambda}{\int_0^\infty G_{\lambda,i} d\lambda} \\ \varepsilon &= \frac{1}{E_{\lambda b}} \int_0^\infty \varepsilon_\lambda E_{\lambda b} d\lambda \\ \rho_r &= \frac{G_r}{G_i} = \frac{\int_0^\infty G_{\lambda,r} d\lambda}{\int_0^\infty G_{\lambda,i} d\lambda} \end{aligned}\right\} \quad (9)$$

Where α_λ and ε_λ are the absorptance and emmitance at specific wave length λ, respectively and $G_{\lambda,i}$ is the incident radiant energy at specific wave length λ. $E_{\lambda,b}$ is the radiant energy emitted by black body at specific wave length. The subscript r and i represents reflected and incident, respectively.

Both absorptivity and emissivity are surface properties while reflectivity is subjected by the angular distribution of incident radiant energy and distribution of wave length. The prediction of collector performance requires the knowledge of absorptivity, emissivity and reflectivity. For a surface maintained at temperature T, the total radiation from the surface is the sum of emitted and reflected which can be written:

$$I_{surface} = I_{emitted} + I_{reflected} \tag{10}$$

The emitted and reflected intensities are:

$$I_{emitted} = \varepsilon I_{Surface}$$
$$I_{reflected} = \rho_r I_{surface}$$

But From Kirchhoff's law, a surface emits equal amount of energy that it absorbs to keep it thermal equilibrium with the surrounding:

$$\varepsilon = \alpha = 1 - \rho_r \tag{11}$$

Equation (11) can be considered as a statement of conservation of energy. The incident energy from any direction is either reflected or absorbed so that

$$\rho_r + \alpha = \rho_r + \varepsilon = 1 \tag{12}$$

4.1.3. Selective Surfaces

Collector absorbers are expected to have a high absorptance for radiation in solar spectrum. They can also lose energy by combination of heat transfer mechanisms including thermal radiation from the absorbers. Therefore, it is important to design a surface for minimum energy loss by thermal radiation. Flat plate collector working temperature is less than 473K and emits a thermal radiation of greater than 3μm wavelength while the solar radiation from is less than 3μm. Thus, the wavelength range of the emitted radiation overlaps only slightly the solar spectrum. From this, it is possible to devise a surface having high solar absorptance and low long-wave emissivity, that is, selective surface (Duffie & Beckman, 1991).

The idealized semi-gray material can be considered as an ideal surface which is gray for solar radiation but different properties for thermal radiation greater than 3μm and this wavelength is called a cut-off wavelength. For this idealized surface, the reflectivity below the cutoff wavelength λ_c is very low. For opaque surface $\alpha = 1 - \rho_r$, so this range α is very high. At wavelength greater than λ_c the reflectivity is nearly unity, and since $\alpha = \varepsilon = 1 - \rho_r$, the emissivity in this range is low.

Real surfaces do not have a well defined critical wavelength λ_c or uniform properties in short and long wavelength ranges. There are several methods of forming selective surfaces. Some of the methods are coating with high absorptivity, interference filters, grooving or pitting the surface to create cavities of dimensions near the cut off wavelength, and directional selectivity. The long wave emissivity versus the reduction in solar absorptivitye, the cost factor to achieve this selectivity, as well as the fact that the surface are usually exposed to oxidizing and corrosive atmosphere and operate at elevated temperature, are the major factors in selecting the material and the technology adopted in the manufacturing of the absorber unit. In flat plate collectors, it is generally more critical to have high absorptance than low emissivity. Coating thickness should give the best combination of these two variables.

4.1.4. Transmittance–Absorptance Product

The amount of radiation incident on the plate depends on the transmittance of the cover τ. Of the radiation passing through the cover system and incident on the plate, some are absorbed and some are reflected back to the cover. However, all this radiation is not lost since some of it return back to the plate. And the resultant transmittance -absorptance can be generalized as (Duffie & Beckman, 1991):

$$(\tau\alpha) = \tau\alpha\sum_{n=0}^{\infty}\left[(1-\alpha)\rho_r\right]^n = \frac{\tau\alpha}{1-(1-\alpha)\rho_r} \tag{13}$$

Where n is the number of reflection inside the collector. For most practical flat plate solar collectors, it is approximated as

$$(\tau\alpha) = 1.01\tau\alpha \tag{14}$$

$(\tau\alpha)$ is also depend on the incidence angle of the radiation θ. The dependency is pronounced for $\theta >$ 45^0

4.1.5. Absorbed Solar Radiation

The evaluation of solar collector efficiency requires information on the solar energy absorbed by the collector absorber. The solar absorbed on a tilted collector can be defined in terms of the inclination angle , transmittance –absorptance product, the total global radiation on the surface and the absorbed radiation S can be generalized as

$$S = I_b\left(\frac{\cos\theta}{\cos\theta_z}\right)(\tau\alpha)_b + I_d(\tau\alpha)_d\left(\frac{1+\cos\beta}{2}\right) + \rho_g(I_b+I_d)(\tau\alpha)_g\left(\frac{1-\cos\beta}{2}\right) \tag{15}$$

Where $\left(\frac{1+\cos\beta}{2}\right)$ and $\left(\frac{1-\cos\beta}{2}\right)$ are the view factors from the collector to the sky and from the collector to the ground, respectively. The subscripts *b, d,* and *g* represent beam, diffuse, and ground respectively.

4.2. Modeling of Liquid Heating Flat Plate Solar Collector

In the design of solar systems, it is the thermal performance of the system which determines the total efficiency. Physical and mathematical modelings are the important steps in engineering problem solving methods. Flat plate solar collectors have been extensively studied and important formulations are developed and experimentally validated. The formulations of flat plate solar collector in this study are based from Duffie & Beckman (1991).

Modeling of flat plate collector includes both optical and thermal modeling. The solar energy absorbed by the absorber plate is distributed to useful heat and thermal loss. Thermal loss can be through the top, side bottom and edges of the collector system. Figure 5 shows the principle of possible thermal loss of a typical flat plate collector. The common methods of heat loss are infrared radiation exchanges, convection heat loss and conduction through the insulations.

Infrared Radiation Exchanges: this is one of the main heat loss methods of flat plate solar collectors. The exchange is between

- the cover and the sky,
- the cover and the ground,
- the absorber and the sky, and
- the absorber and the sky,

Convective heat loss: the convective heat losses are due the air in the cover and absorber gap and the ambient air.

Conduction heat losses: heat loss by conduction in the collector is due to bottom, side and edges of the collector system.

Single-Node Modeling

It is most common method to estimate the absorbed solar radiation and the thermal behavior of conventional flat plate collector by a single-node. Single-node modeling is representing all type of heat loss by a single overall heat transfer coefficient. In this thermal analysis of flat plate collector, substantial assumption has been considered to simplify the thermal and optical behavior of the collector. Though transient and unpredicted nature of solar energy in a given period, steady state heat transfer condition is the initial concept used in the modeling of conventional flat plate collector. In a steady state single-node model of flat plate collector, the energy balance includes the energy gain by the moving fluid, the thermal

loss and the optical losses. Illustrating the temperature distribution is useful to deal with single node modeling. Figure 6 shows two dimensional temperature distribution of the absorber. Some of the energy absorbed by the absorber is conducted and transferred to the fluid which results a temperature gradient in the absorber in the x-axis. The heat transferred to the fluid increases the temperature of the fluid which also result a temperature gradient in the y-axis. To get the mathematical model which can describe the temperature behavior of the collector, the following assumptions simplifies the complexity with minimum error (Duffie and Bekeman, 1991).

- Temperature gradient through the cover is negligible
- There is one-dimensional heat flow through the back and side insulation and through the cover system
- There is no absorption of solar energy by cover
- There is negligible temperature drop through the cover
- The cover is opaque for infrared radiations
- The sky can be considered as a blackbody for long-wavelength radiations at an equivalent sky temperature
- Temperature gradient around the tubes, through the fluid is negligible
- The temperature gradient in the direction of flow and between the tubes can be treated independently
- Properties are independent of temperature
- Loss through front and back are to the same temperature
- Dust and dirt on the collector are negligible
- Shading of the collector absorber plate is negligible

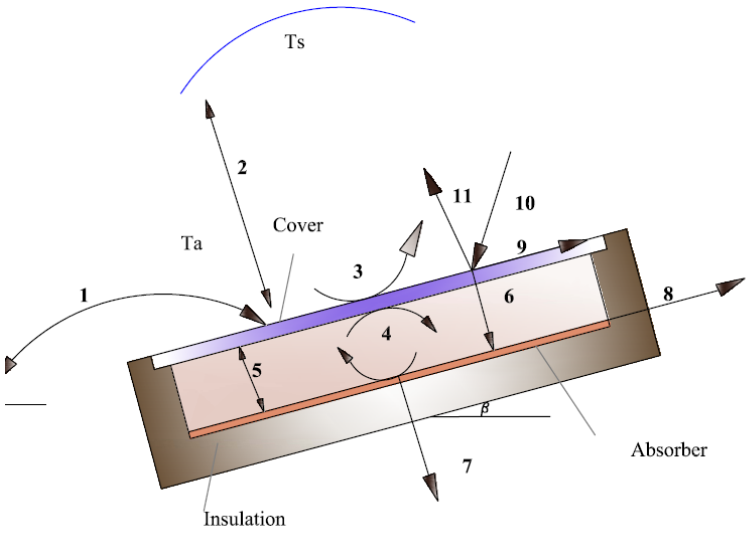

Figure 5. Thermal performance of typical flat plate solar collector

Where:

- Radiation exchange between ground and cover, 1
- Radiation exchange between sky and collector cover,2
- Ambient wind convection heat loss, 3
- Convection heat exchange between absorber plate and cover by the hot air in the gap, 4
- Radiation exchange between cover and absorber plate, 5
- Absorbed solar radiation by the absorber plate, 6
- Heat loss to insulations, edges and sides, 7
- Net useful heat, 8
- Solar Radiation absorbed by the cover, 9
- Total solar radiation incident, 10

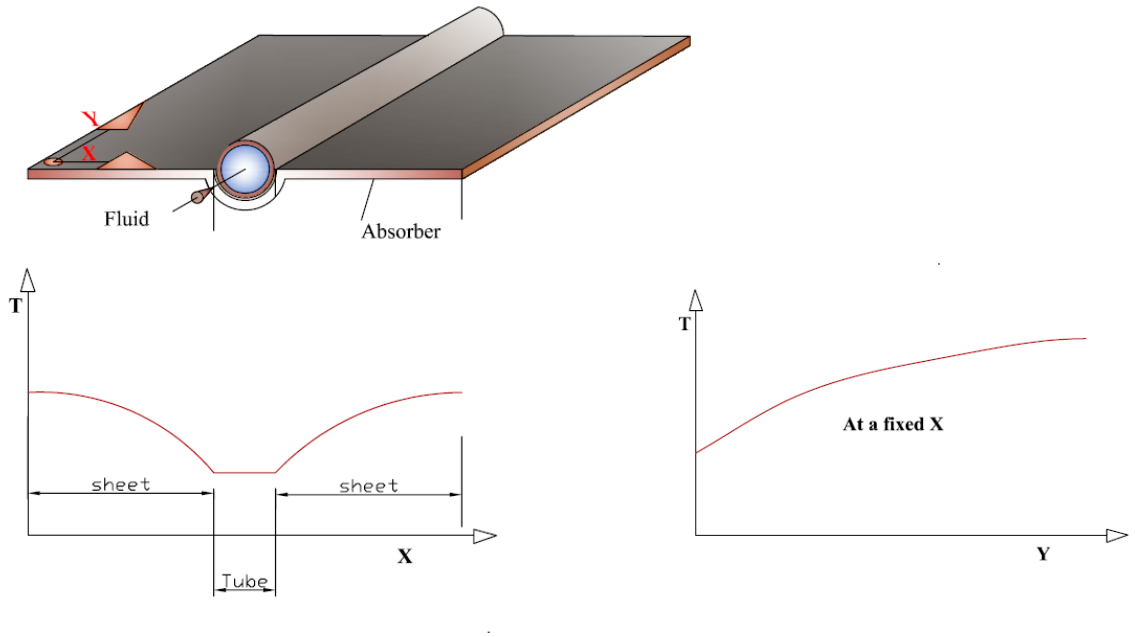

Figure 6. Temperature distribution on an absorber plate

In the process of single node modeling, finding a representative overall transfer coefficient is the important task. Figure 7 shows the thermal resistance network to calculate the total heat transfer coefficient, U_L for a single cover flat plate solar collector.

From the thermal network shown in Figure 7 the top heat loss can be written,

$$q_{loss,top} = h_{c-a}(Tc - Ta) + h_{r,c-a}(Tc - Ta)$$
$$= h_{p-c}(Tp - Tc) + h_{r,p-c}(Tp - Tc) \quad (16)$$

Whereas the radiation heat transfer coefficients can be calculated:

$$h_{r,p-c} = \frac{\sigma\left(T_p + T_c\right)\left(T_p^{\,2} + T_c^{\,2}\right)}{\frac{1}{\varepsilon_p} + \frac{1}{\varepsilon_c} - 1}$$

$$h_{r,c-a} = \frac{\sigma\left(T_c + T_s\right)\left(T_c^{\,2} + T_s^{\,2}\right)}{\frac{1}{\varepsilon_c} + \frac{1}{\varepsilon_s} - 1}$$

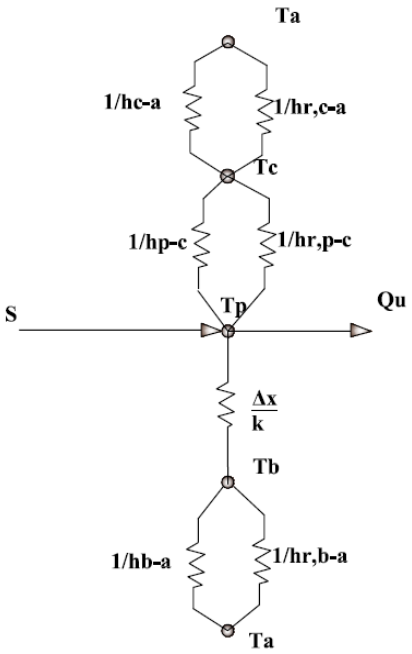

Figur 7. Thermal network for one cover flat plate collector

Where σ is the Stefan-Boltzman constant and is equal to $5.6697x10^{-8} W/m^2k^4$, ε is the emissivity and Ts is the sky temperature. The sky temperature can be calculated using the correlation (Duffie and Beckman, 1991)

$$T_s = 0.0552 T_a^{1.5}$$

The convective heat transfer coefficient between the absorber and the cover can be calculated using the concept of natural convection between flat parallel plates. The free convective heat transfer is related to

two or three dimensionless parameters: Nusselt number Nu; the Rayleigh number Ra; and the Prandtle number Pr.

$$Nu = \frac{h_{c,p-c} L}{k} \tag{17}$$

$$Ra = \frac{g\beta' \Delta T L^3}{v\alpha_d} \tag{18}$$

$$\Pr = \frac{v}{\alpha_d} \tag{19}$$

Where

L – Plate spacing , characterstic length
ΔT – temperature difference between plates

The relationship between the Nusselt number and Rayleigh for tilt angle β from 0^o to 75^0 is suggested by Hollands et al. (1976).

$$Nu = 1 + 1.44\left[1 - \frac{1708(\sin 1.8\beta)^{1.6}}{Ra\cos\beta}\right]\left[1 - \frac{1708}{Ra\cos\beta}\right]^{+} + \left[\left(\frac{Ra\cos\beta}{5830}\right)^{1/3} - 1\right]^{+} \tag{20}$$

The calculation of wind convective heat transfer coefficient needs extra fourth dimensionless parameters called Reynolds (Re) number defined as

$$\mathrm{Re} = \frac{\rho u L_c}{\mu} \tag{21}$$

Where Lc is the length of the collector.

For wind convection, Duffie and Beckman suggested to use the Sparrow model for Reynolds number $2x10^4$ to $9x10^4$:

$$Nu = 0.86\,\mathrm{Re}^{1/2}\,\mathrm{Pr}^{1/3} \qquad 2x10^4 < \mathrm{Re} < 9x10^4 \tag{22}$$

And for flow over a very wide flat plate collector with zero angle of attack, Pohihausen relation is recommended

$$Nu = 0.94\,\mathrm{Re}^{1/2}\,\mathrm{Pr}^{1/3} \qquad \mathrm{Re} < 2x10^4 \tag{23}$$

Therefore, the total top heat transfer coefficient can be calculated:

$$U_t = \left(\frac{1}{h_{p-c} + h_{r,p-c}} + \frac{1}{h_{c-a} + h_{r,c-a}} \right)^{-1} \tag{24}$$

Taking the equivalent thermal resistance, U_L – total heat transfer coefficient

$$U_L = U_t + U_b + U_e \tag{25}$$

Assuming the temperature difference between the bottom surface temperature and ambient is zero, bottom heat transfer coefficient, Ub is

$$U_b = \frac{k}{L} \tag{26}$$

where L is the insulation thickness at the bottom and k is the conductivity of the insulation

Duffie &Beckman (1991) recommended the edge heat transfer coefficient, Ue as

$$U_e = \frac{(UA)edg}{Ac} \tag{27}$$

Where - UA is the loss coefficient area product and Ac is the collector area

The calculation of overall heat transfer coefficient for steady state model doesn't consider the capacitance of any of the collector system during the course of operation. Figure 8 shows the single node model with overall heat transfer coefficient.

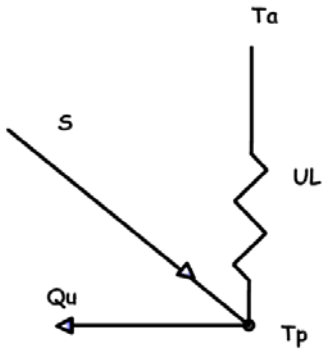

Figur 8. Single node representation of flat plate collector

For mathematical modeling of collector fin temperature distribution, lets us to find the optimum fin length and effectiveness of the fin for heat transfer to the fluid. To model the heat transfer, we assume for the moment that the temperature gradient along the axis of fluid flow is negligible.

Taking energy balance on the fin element from Figure 9:

$$S dx - U_L dx(T - T_a) + \left[-k\delta \left. \frac{dT}{dx} \right|_x \right] - \left[-k\delta \left. \frac{dT}{dx} \right|_{x+dx} \right] = 0$$

This gives

$$\frac{d^2T}{dx^2} = \frac{U_L}{k\delta}\left(T - T_a - \frac{S}{U_L} \right) \tag{28}$$

Boundary conditions:

$$\left. \frac{dT}{dx} \right|_{x=0} = 0, \quad T\big|_{x=(W-D)/2} = T_b$$

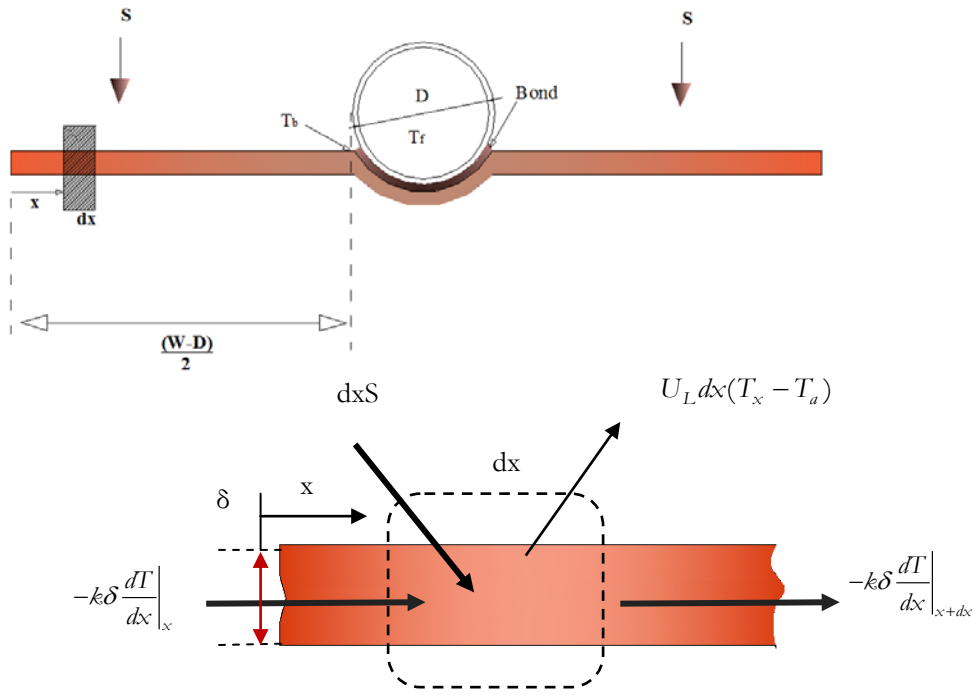

Figure 9. Fin dimension and energy balance on fin element

Solving analytically the above second order differential equation, the flux to the fluid is given by

$$q_{fin} = (W - D)\left[S - U_L\left(T_b - T_a \right) \right] \frac{\tanh m(W - D)/2}{m(W - D)/2} \tag{29}$$

Where

$$m = \sqrt{U_L / k\delta}$$

Introducing fin efficiency, F

$$q_{fin} = (W - D)F\left[S - U_L\left(T_b - T_a\right)\right] \tag{30}$$

Where

$$F = \frac{\tanh m(W-D)/2}{m(W-D)/2}$$

Where F is the fin efficiency

The value of the width is selected by optimization of the fin efficiency and the value of total heat transfer coefficient. The useful gain of the collector includes the energy collected above the tube region given by:

$$q_{tube} = (D)\left[S - U_L\left(T_b - T_a\right)\right]$$

Therefore the total heat gain per length of tube is

$$q_u = \left[(W - D)F + D\right]\left[S - U_L\left(T_b - T_a\right)\right] \tag{31}$$

Bond and Fluid Resistance: The useful gain defined above by the tube is limited by the bond resistance and the fluid resistance in the tube. Poor bonding between the collector and the tube limits the amount of heat delivered to the fluid. According to Duffie and Beckman (1991), the total heat delivered per length of the tube is defined as:

$$q_u = \frac{T_b - T_f}{\frac{1}{h_f \pi D_i} + \frac{1}{C_b}} \tag{32}$$

where D_i is the internal tube diameter, h_f is the convective heat transfer coefficient in the tube and C_b is the bond conductance. The bond conductance can be estimated from the concept of thermal conductivity kb, the average bond thickness γ and the bond width b.

$$C_b = \frac{k_b b}{\gamma}$$

For better heat transfer, the bond conductance is recommended to be higher than 30 W/m ^{o}C.

To simplify the problem of finding the base temperature T_b, which is difficult to measure, collector efficiency factor F' is introduced which includes bond and fluid resistances. The heat gain per unit length of the tube is now defined in terms of the fluid temperature:

$$q_u = WF'\left[S - U_L\left(T_f - T_a\right)\right] \tag{33}$$

Where the collector efficiency factor F' is

$$F' = \frac{1/U_L}{W\left[\frac{1}{U_L\left[D+(W-D)F\right]}+\frac{1}{C_b}+\frac{1}{\pi D_i h_f}\right]}$$

The collector efficiency factor is a constant for any collector design. However, U_L, C_b, h_{fi}, and F are variable with temperature.

The temperature distribution in the flow direction is also a factor in the total heat transfer to the fluid. The temperature gradient created in the direction of the fluid flow increase the heat loss from the collector. Considering heat and mass transfer in the fluid tube, the relation between the outlet and inlet temperature of fluid in a single collector is given by Duffie and Beckman (1991) as

$$\frac{T_{fo}-T_a-S/U_L}{T_{fi}-_a-S/U_L} = e^{\left(-A_c U_L F'/\dot{m}Cp\right)}$$

Where T_{fo} is the outlet fluid temperature, T_{fi} inlet fluid temperature, Ac collector area, m is the mass flow rate in the tube, and C_p is the heat capacity of the fluid.

Collector heat removal factor F_R is also the most common method to define the actual energy gained in the collector with the heat gained as if the absorber temperature is equal to the inlet fluid temperature.

$$F_R = \frac{\dot{m}C_p}{A_c U_L}\left[1-e^{\left(-A_c U_L F'/\dot{m}Cp\right)}\right] \tag{34}$$

For graphical expression, a collector flow factor F" is defined

$$F'' = \frac{F_R}{F'} = \frac{\dot{m}C_p}{A_c U_L F'}\left[1-e^{\left(-A_c U_L F'/\dot{m}Cp\right)}\right] \tag{35}$$

The flow factor only depends on the dimensionless variable the heat capacitance rate $\dot{m}Cp/AcU_LF'$. F_R is equivalent to the effectiveness of conventional heat exchanger defined as the actual heat transfer to the maximum possible. In solar collector, the maximum heat transfer occurs when the collector is at fluid inlet temperature so that heat loss is minimum value. Therefore, the heat removal factor times the maximum possible useful energy gained gives the actual possible useful energy gained.

$$Q_u = A_c F_R\left[S-U_L(T_i-T_a)\right] \tag{36}$$

This equation applies for liquid heating flat plate collectors. The efficiency of a collector can be then defined:

$$\eta = \frac{Q_u}{IA_c} \tag{37}$$

Where I is the solar radiation in W/m^2

5. Mathematical Modeling of Solar Collector for Water Heating

5.1. Mathematical Modeling of Natural Circulation Solar Water Heating

Natural circulation solar water heaters have got a great interest because of their simple design and no external power is required for the system. The advantage of this system is that it can be used in rural areas where grid electricity is not possible. In the system, the heat transfer fluid (water in this case) circulates from the collector to the hot water storage by buoyancy created by temperature difference. Apart from the climatic parameters, the system performance is subjected to system design geometries. Numerous studies have been done on the theoretical and experimental study of this type of solar water heater. Huang (1980) theoretically studied the impact of tanker height on the performance of natural circulation solar collector and found for low flow resistance and heat loss, the mean collector efficiency is independent of tanker height and solar radiation. Sodha(1981) theoretically studied the same type solar collector and found the collector system efficiency greatly depend on the height of the tanker from the collector and collection temperature. Gupta and Garg (1968) has experimentally investigated the impact of tanker height from top collector end and found that the efficiency and the mean tanker temperature was not affected by the height of the tanker from the solar collector. Siddiqui (1997) studied the effect of solar flux in heat transfer and fluid flow in closed loop natural circulation solar water heater and found the average heat transfer coefficient increases with solar flux due to the high temperature difference between the mean fluid temperature and ambient temperature. The Nusselt number was also found increased for high solar flux and the Reynolds number varies according to the variation of solar flux. Zerrouki et.al (2002) experimentally investigated the performance natural circulation solar water heater and found a comparable result when compared with related works. In the present study, a small natural circulation solar collector is theoretically and experimentally investigated for water heating. The collector system is designed so the mean tanker height from ground is the same as the top collector end height from the ground. The performance of this collector is also compared with heat pipe solar collectors with natural convective condenser. Figure 10 shows both the prototype design and physical model of the system. Mathematical model of single phase thermosyphon (natural circulation) water heater is developed based on Close(1965), Gupta and Garg (1968) and Ong (1974).

Mathematical model for Mean Tanker Temperature

From Figure 10(b), the instantaneous heat and mass balance of the system can be written as

$$\dot{m} c_p (T_5 - T_3) = FA_c [\ S\ -\ U_L (\ T_m - T_a)\ ] - \ (\sum_{i=1}^{n} m_{ci} c_{ci}) \frac{dT_c}{dt} - m_{pip} c_{pip} \frac{dT_{pip}}{dt}\ - U_{pip} (\ T_{pip} - \ T_a)$$

(38)

Where F is the collector efficiency factor multiplied by the width of the collector

$$F = WF'$$

T_m- is the mean fluid temperature in the collector

$$\dot{m} c_p (T_5 - T_3) = \ m_T c_p \frac{dT_T}{dt} + m_{WT} c_p \frac{dT_n}{dt}\ + U_T (\ T_n - \ T_a)$$

(39)

Where m_T is the mass of the tanker, m_{WT} is the mass of water in the tanker and T_T is tanker temperature.

For computation of losses due capacities the body temperature of the tanker and the collector are assumed to be equal to the respective water temperature. Thus putting $T_c=T_m$, $T_T=T_n$ and $T_f=T_p$

$$\dot{m} c_p (T_5 - T_3) = FA_c\ S\ -\ [F A_c U_L (\ T_m - T_a) + (\sum_{i=1}^{n} m_{ci} c_{pi} \frac{dT_m}{dt} + m_{pip} c_p \frac{dT_{pip}}{dt}\ + U_{pip} (\ T_{pip} - \ T_a)]$$

(40)

$$\dot{m} c_p (T_5 - T_3) = \ (m_T c_{pT} + m_{WT} c_{pWT}) \frac{dT_n}{dt}\ + U_T (\ T_n - \ T_a)$$

(41)

On the base of experimental observation, the mean temperature in the tank is the same as the mean temperature in the absorber (Close, 1965). This also holds for the pipe. Putting $T_m=T_n=T_p$ and solving C_0 in equation (40) and (41), the equation for mean system temperature T_n is given during the sun hours

$$C \frac{dT_n}{dt} + U(T_n - T_a) = FA_c S$$

(42)

$$C = \sum_{i=1}^{n} m_{ci} c_{pi} + m_{pip} c_{pip} + m_T c_{pT} + m_{WT} c_{pWT}\ ;\ U = \ FA_c U_L + \ U_{pip} + \ U_T .$$

To investigate the system temperature at night (S=0), the equation (42) has to be uncoupled. Therefore, the absorber mean temperature and tank temperature are:

$$C_1 \frac{dT_m}{dt} + U_1 (T_m - T_a) = 0$$

(43)

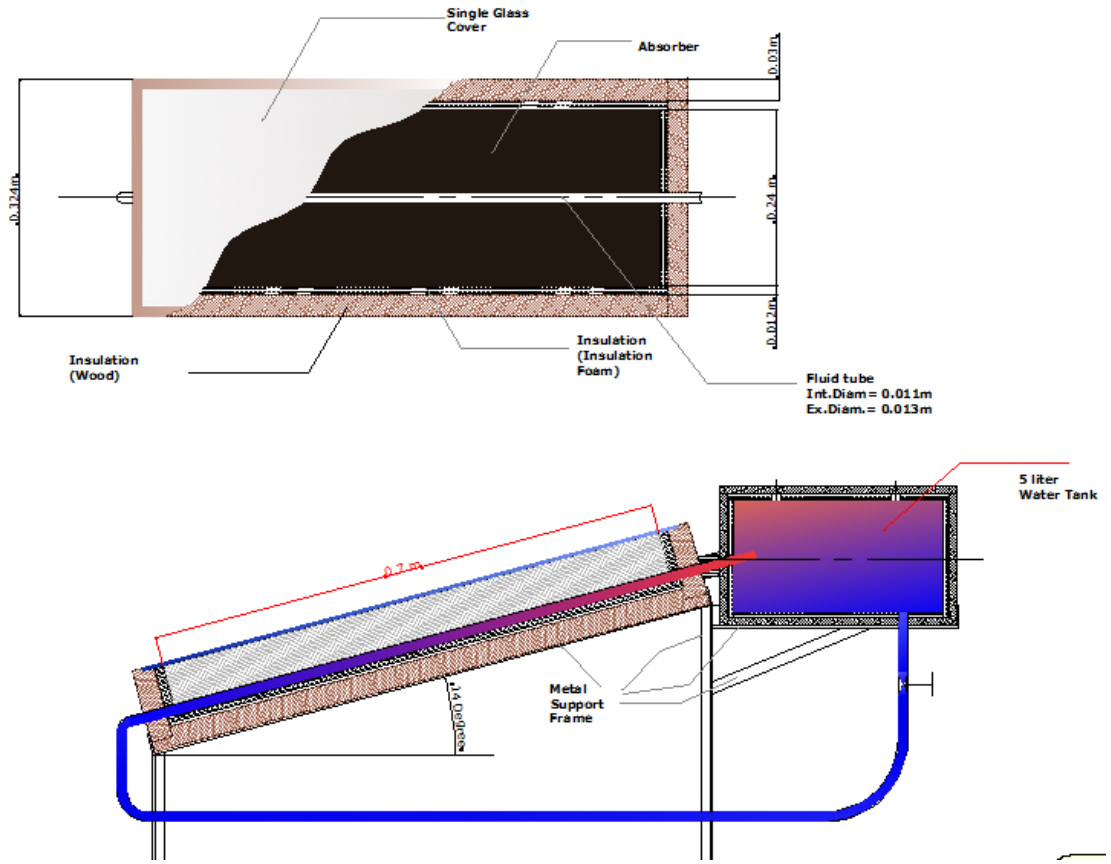

(a)

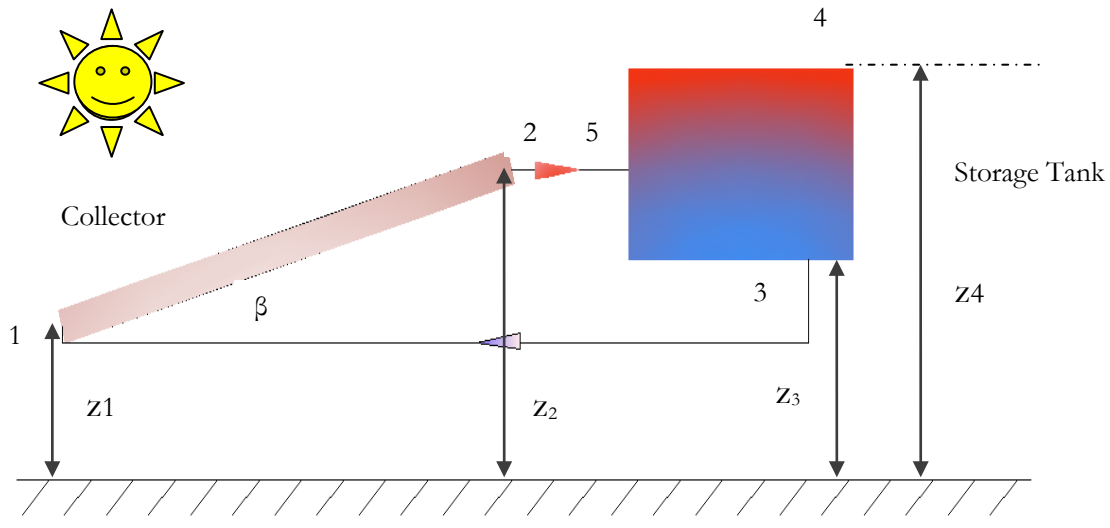

(b)

Figur 10. (a) Natural circulation solar collector design (b) physical model for natural circulation collector

$$C_2 \frac{dT_n}{dt} + U_2(T_n - T_a) = 0 \tag{44}$$

$C_1 = C - C_2$, $C_2 = m_T c_{pT} - m c_{pWT}$, $U_1 = U - U_2$, $U_2 = U_T$

Equation (42),(43) and (44) are first order non-homogeneous differential equations which can be solved numerically. Equation (42) is used to compare collector efficiency with different type of collector types.

Mass Flow Rate

The instantaneous mass flow rate can be calculated using the knowledge of pressure drop. Temperature distribution in the collector circuit creates a density difference which results a pressure head for the fluid to flow in the circuit. The pressure head developed due to density difference is equal to the pressure head loss due to friction. Thus:

$$P_\rho = P_{fr} \tag{45}$$

Following Close (1965), the specific gravity variation due to temperature can be expressed by quadratic polynomial

$$sp.gr = AT^2 + BT + C \tag{46}$$

Where A=*-1.25x10-6, B=5.83x10-5* and *C=0.99967*

The thermal pressure head developed can be written using the mean tanker temperature as

$$P_\rho = \frac{(T_2 - T_1)}{2}\left(2T_n A - B\right) f(z) \tag{47}$$

Where $f(z) = (z_2 - z_1) - \frac{(z_5 - z_3)^2}{z_4 - z_3}$

Assuming negligible velocity pressure head loss at bends and other restriction for this specific work, the pressure head loss due to friction in the flow circuit can be found using Darcy Weisbach equation

$$P_{fr} = \frac{flu^2}{2gd_t} \tag{48}$$

where l is the total flow circuit length and for laminar flow, f=0.035

Rewriting the fluid velocity in terms of mass flow rate

$$u = \frac{4\dot{m}}{\rho\pi d_t^2}$$

Substituting u in equation (48)

$$P_{fr} = \frac{8 fl \left(\dot{m}\right)^2}{g\pi^2 \rho^2 d_t^{\,5}} \tag{49}$$

equating equation(47) and (49) and rearranging

$$\left(\dot{m}\right)^2 = \left[\frac{\left((T_2 - T_1)\left(2T_n A - B\right) f(z)\right) g\pi^2 \rho^2 d_t^{\,5}}{16 fl}\right] \tag{50}$$

From Figure 10,

$$\left(T_2 - T_1\right) = \left(T_5 - T_3\right)$$

Considering equation (41)

$$\left(\dot{m}\right)^3 = \left[\frac{\left((T_2 - T_1)\left(2T_n A - B\right) f(z)\right) g\pi^2 \rho^2 d_t^{\,5}}{16 flc_p}\right]$$
$$(T_2 - T_1) = \left[(m_T c_{pT} + m_{WT} c_{pWT})\frac{dT_n}{dt} + U_T(\,T_n - T_a)\,\right] \tag{51}$$

Mean temperature of tanker can be numerically computed from equation (42) so that the mass flow is obtained.

System Efficiency

Collector performance is measured by collection efficiency which is defined as the ratio of useful energy collected to the solar radiation on the collector area in a specified time interval (Duffie and Beckman, 1991). Collection efficiency (η) is a single parameter that combines collector and system characteristics.

$$\eta = \frac{\int Q_u dt}{A_c \int I dt}$$

Where Q_u is useful heat. Instantaneous efficiency of the collector can be calculated:

$$\eta_i = \frac{Q_u}{A_c I} = \frac{F[S - U_L(T_n - T_a)]}{I} \tag{52}$$

5.2. Mathematical Modeling of Heat Pipe Solar Collectors

The transient nature of solar energy during operation time makes heat pipe to work in transient heat transfer. This is more pronounced in batch type of solar water heaters where the temperature of the

condensing media increases in time. Figure 11 shows thermal resistance –capacitance model of heat pipe integrated solar water heater. As can be seen in the figure, the heat pipe can be modeled using three capacitance and five thermal resistances. Hussein et al (1999) and Hassein (2007) have studied the performance of wickless heat pipe for solar water heating using transient heat transfer models and optimized different system parameters. On the other side, most studies on heat pipe application for solar application consider one-node model adapted from Duffie and Beckman (1991) where the heat pipe fluid inside works wholly saturated.. Mathioulakis and Belessiotis (2002) investigated both theoretically and experimentally new ethanol heat pipe solar collector for water heating by assuming a steady state operation of heat pipe fluid at saturated pressure and temperature and no capacitance in the heat pipe sections. The evaporation heat transfer resistance has been considered in the study. But no information was given concerning condensation and vapor heat transfer resistances. Chen et al.(2011) has also studied a two phase thermosyphon solar collector with alcohol as a working fluid both theoretically and experimentally. Thermal resistance –capacitance model was developed and working fluid capacitance was assumed negligible. The thermal resistance of the working fluid vapor resistance was found very small compared to evaporation and condensation thermal resistances. Tardy and Sami (2009) and Ismail and Abogderah (1998) have also studied heat pipe for thermal storage and solar collector, respectively. Saturated temperature and pressure were assumed in the heat pipe working fluid. Only evaporation and condensation thermal resistances have been considered in their models. The working fluid capacitance and vapor thermal resistance are assumed negligible in this study too. Only evaporation and condensation thermal resistances are considered as heat pipe thermal resistances.

Two phase thermosyphon solar collector with distilled water working fluid was investigated both numerically and experimentally and was found to have small temperature variation on absorber, cover and heat pipe during the test hours (Taherian.et al., 2011) This can help as to assume that the collector and the heat pipe works in quasi-steady state condition. Moreover, the following assumptions are considered in mathematical models of heat pipe solar collectors:

- Heat pipe working fluid is assumed at saturated temperature and pressure during operation
- The vapor thermal resistance is assumed negligible
- The thermal capacitance of evaporator, condenser and working fluid are ignored
- The adiabatic section of the heat pipe is well insulated so that heat loss is assumed negligible
- There is no temperature gradient in the cover of the collector
- Since the heat pipe works at saturation temperature , temperature gradient along the longitudinal direction of evaporator is neglected
- Temperature gradient on the perimeter of the absorber, across the absorber plate thickness, and across the heat pipe thickness is neglected
- The solar collector and the heat pipe works at quasi-steady state

- The back, sides and edges of the collector are well insulated and the thermal resistance is only by insulation. The same is true for the water tanker.
- No temperature gradient in along condenser and evaporator sections

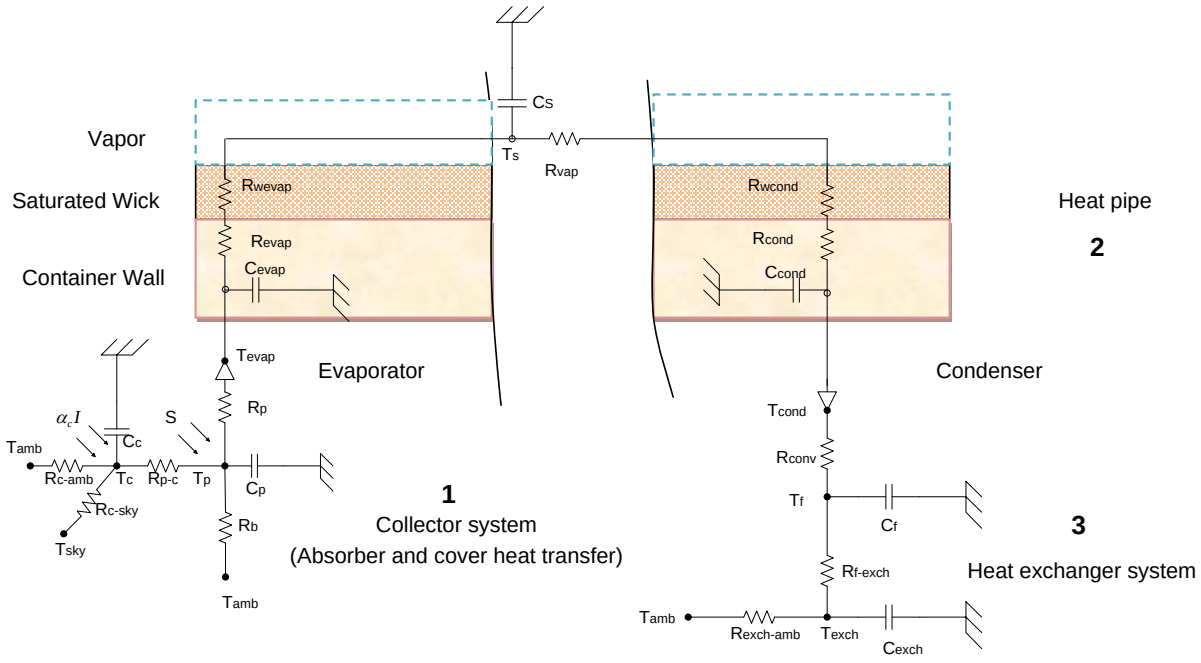

Figur 11. Integrated thermal resistance-capacitance heat pipe solar collector model

5.2.1. Mathematical Modeling of Heat Pipe Solar Collector with Natural Convective Condenser

Natural convective heat pipe or two-phase thermosyphon solar collectors have been studied by several researchers. Chun et al. (1999) has experimentally studied heat pipe solar collector for water heating. The condenser section of the heat pipe was directly inserted to the storage tanker in which natural convective heat transfer happens. Three heat pipe working fluids: water, acetone, methanol and ethanol were tested for their performance and no appreciable difference was seen on their performance. The performance of the tested heat pipe collector was found to have a better performance compared to conventional natural circulation solar water heater.

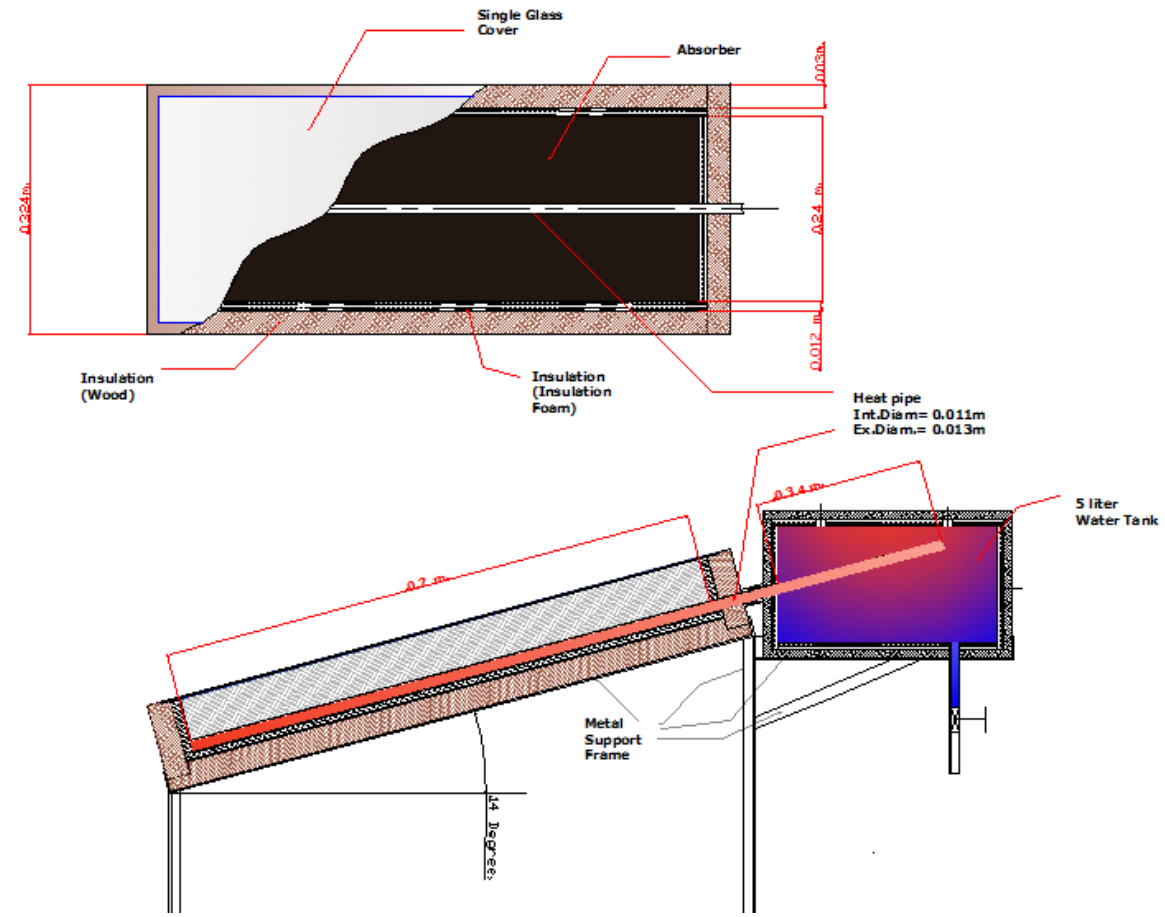

(a)

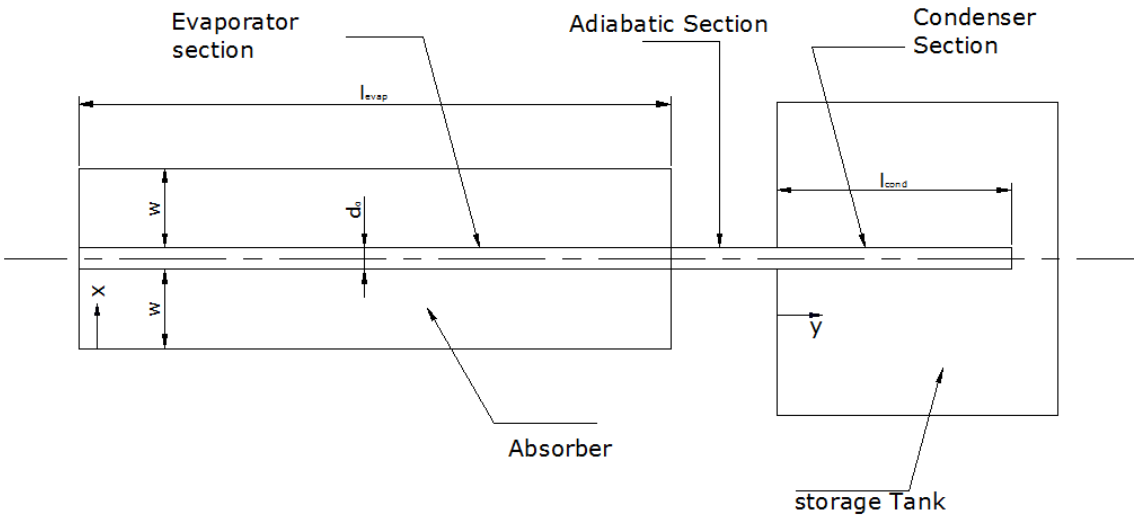

(b)

Figur 12. (a) Heat pipe solar collector with natural convective condenser design (b) physical model for energy balance

Considering a single–node model discussed above for the heat pipe solar collector, the energy balance in the tanker can be written as follows:

$$V_w \rho_w c_w \frac{dT_w}{dt} = \pi d_o l_{cond} h_{eff} (T_{hp} - T_w) - U_{\tan} A_{\tan} (T_w - T_a) \tag{53}$$

Where $U_{tan}A_{tan}$ is the product of the heat transfer coefficient and the area of the tanker

h_{eff} is the effective heat transfer coefficient in the condenser section of heat pipe and can be found

$$h_{eff} = \left(\frac{1}{h_{cond}} + \frac{1}{h_f} + \frac{\delta_{hp}}{k_{hp}} \right)^{-1} \tag{54}$$

Where h_{cond} is the film condensation heat transfer coefficient in the condenser section of the heat pipe and can be found using Nusselt equation

$$h_{cond} = 0.729 \left(\frac{k_l^{\,3} \lambda \rho_l (\rho_l - \rho_v) g \sin\beta}{\mu_l d_i (T_{hp} - T_w)} \right)^{1/4} \tag{55}$$

h_F is the natural convective heat transfer coefficient between the condenser section and the water to be heated and can be found from Nusselt equation(Coulson & Richardson's chemical engineering, volume I , 1999, pp(435), Perry and Green (1999), chemical engineer's handbook section 5, pp 13)

$$\frac{h_f d_o}{k_l} = 1.09 \left(\frac{d_o^{\,3} \rho_l^{\,2} g \gamma (T_{hp} - T_w) C_p}{\mu_l k_l} \right)^{1/5} \tag{56}$$

The system instantaneous efficiency can be calculated

$$\eta_i = \frac{Q_u}{A_c I} = \frac{F[S - U_L (T_{wi} - T_a)]}{I} \tag{57}$$

5.2.2. Mathematical Modeling Heat Pipe Solar Collector with Forced Convective Condenser

Forced convective condensers can be designed either in cross flow or parallel flow heat exchanger. The efficiency of these condensers has been rarely compared for their performance. These two heat exchangers are manufactured and tested both theoretically and experimentally. Figure (13) and (14) show models for the prototype design for testing of heat pipe solar collector under different condensing mechanisms. The following additional assumptions are considered for this specific case:

- Water tubes are well insulated and the heat loss is neglected
- Condensing water flow is assumed constant

- The heat exchanger is well insulated to consider the heat loss is only due to conduction through insulations.
- The holes bored in the collector system for piping and measurement system have no special effect on the insulation system in the sides of the collector and the heat exchanger boxes.
- Cross flow heat exchanger condensing water flows fully perpendicular to the condenser section of heat pipe while fully parallel in parallel heat exchanger
- No temperature gradient along the axis of heat pipe in heat exchangers
- Energy balance mathematical models for cover and absorber plate are the same as discussed in natural convective heat pipe condensers

Considering a single-node model for heat pipe solar collector, the energy balance in the tanker can be written as

$$mc_p \frac{dT_w}{dt} = \pi d_o l_{cond} h_{eff} (T_{hp} - T_w) - U_{eq} A_{eq} (T_w - T_a) \tag{58}$$

Where $U_{eq}A_{eq}$ is the product of overall heat transfer coefficient in the tanker, heat exchangers and tubing and the equivalent area.

$$h_{eff} = \left(\frac{1}{h_{cond}} + \frac{1}{h_f} + \frac{\delta_{hp}}{k_{hp}} \right)^{-1} \tag{59}$$

For flow perpendicular (cross flow heat exchanger) to the heat pipe, the heat transfer coefficient can be found by the following correlation (Coulson & Richardson's Chemical Engineering, volume I, 1999, pp(426-7))

$$\frac{h_f d_o}{k_l} = 0.26(\mathrm{Re}^{0.6}\,\mathrm{Pr}^{0.3}) \tag{60}$$

The outside diameter of the heat pipe is considered for characteristic length

$$h_{cond} = 0.729 \left(\frac{k_l^{\,3} \lambda \rho_l (\rho_l - \rho_v) g \sin\beta}{\mu_l d_i (T_{hp} - T_{cond})} \right)^{1/4} \tag{61}$$

For flow parallel (parallel flow heat exchanger) to the heat pipe section, the heat transfer coefficient can be found by the following correlation (Coulson & Richardson's chemical engineering, volume I, 1999, pp(433))

$$\frac{h_f d_e}{k_l} = 0.027(\mathrm{Re}^{0.8}\,\mathrm{Pr}^{0.33}) \tag{62}$$

The characteristic length is $d_e = D_i - d_o$, where D_i is the internal diameter of the heat exchanger.

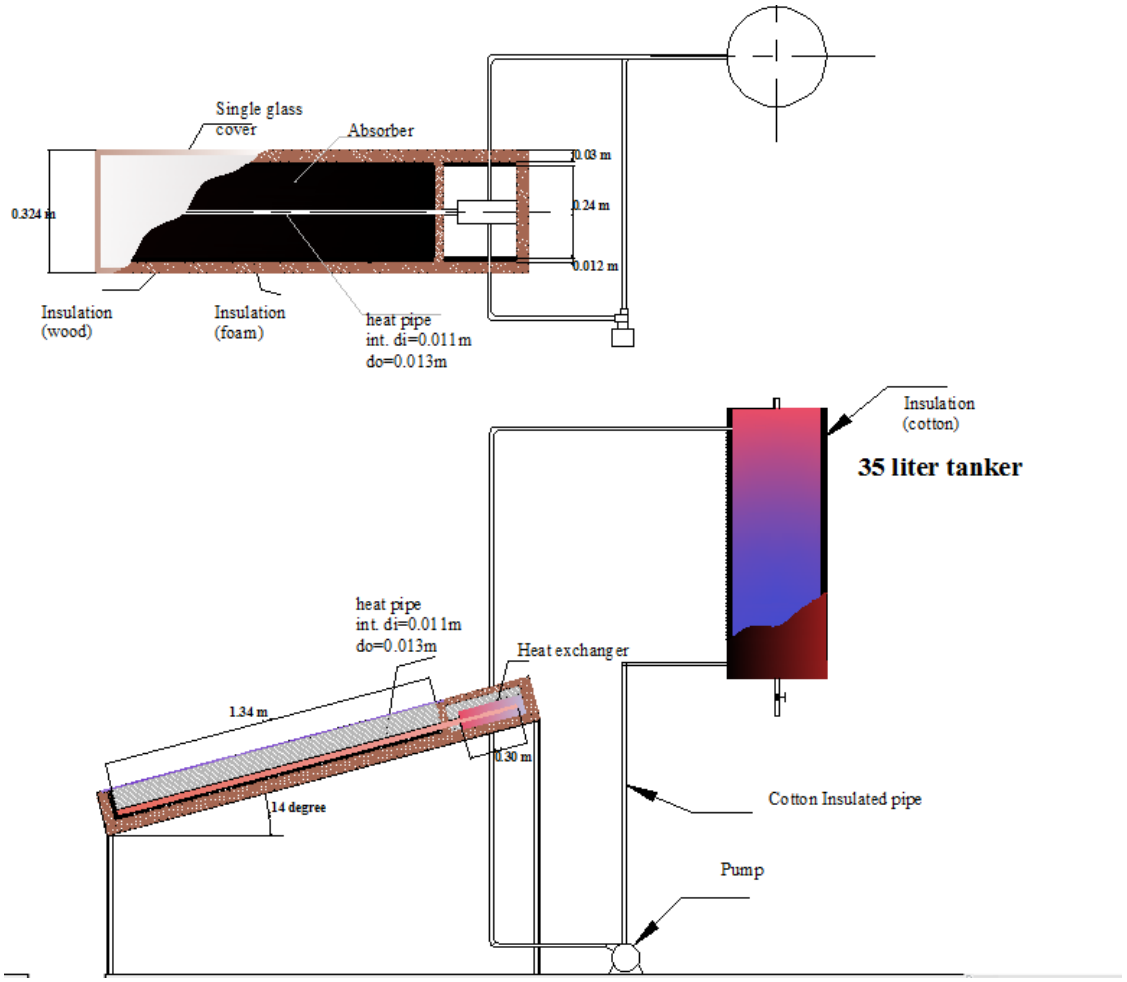

Figur 13. Prototype design of heat pipe solar collector with forced convective condenser

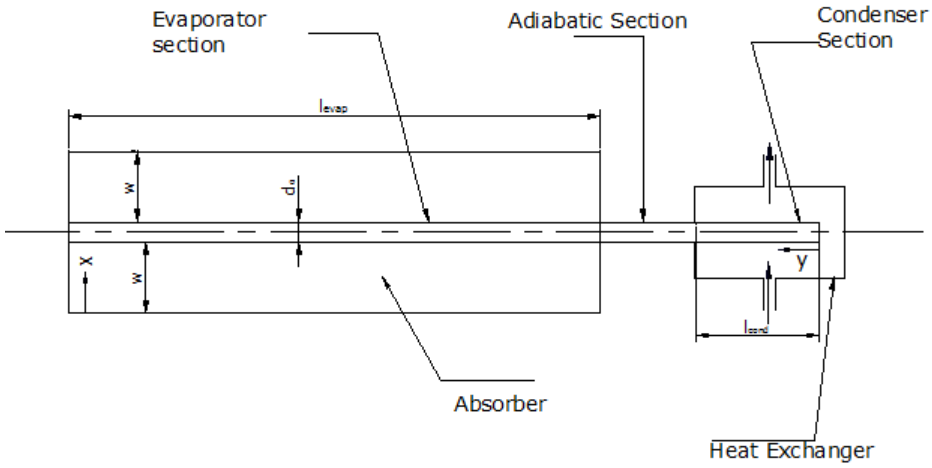

(a)

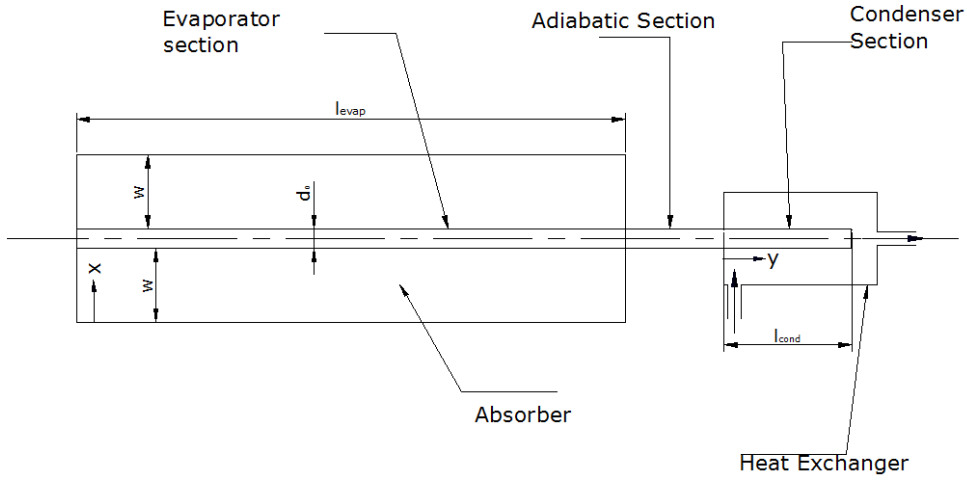

(b)

Figur 14. (a) physical model cross flow heat exchanger, (b) physical model for parallel flow heat exchanger

Initial condition

$$T_w = T_{w0} \qquad \text{at} \quad t = 0$$

Instantaneous efficiency can be calculated:

$$\eta_i = \frac{Q_u}{A_c I} = \frac{F[S - U_L(T_{wi} - T_\infty)]}{I} \tag{63}$$

Matlab codes are developed for numerical solution of ODE problems. The following central difference finite difference method is used to discretize the mathematical equations.

$$\frac{dT}{dt} = \frac{T^{n+1} - T^n}{\Delta t}$$

6. Experiments and Materials

According to the design diagrams shown in Figure 10, 12 and 13, test rings are manufactured to test the performance of natural circulation, natural and forced convective heat pipe solar collectors for water heating. Two collector systems are manufactured with different dimensions based on two successfully manufactured heat pipe dimensions. Manufacturing of heat pipe has been very challenging due to leakage and old vacuum pump available.

6.1. Heat Pipe Manufacturing

Heat pipes are the core component of the project and need careful design and manufacturing. For long life operation, a heat pipe has to be properly designed and sealed for leakage proof. Proper selection of container materials, wick materials and mesh type, working fluid, working pressure and filling ratio play a vital role to attain the required performance of solar collector. Heat pipe manufacturing requires the following basic equipments: Vacuum pump with pressure measuring accessories, copper tube with copper mesh for wick, distilled water for working fluid, calibrated water gage, control valves, connections and sealing devices such as vice and soldering equipments. Figure 15 shows the experimental set up heat pipe manufacturing. The following procedures are followed for manufacturing:

1. Copper tube sizing and wick preparation: copper with 13 mm outside diameter is cut and cleaned thoroughly. A single layer copper wick with 100 mesh size is prepared for insertion.
2. One end of the tube is cramped by a vice and soldered for leakage proof.
3. The pressure gage, vacuum pump, and distilled water filling system are connected
4. The pump evacuates the pipe to the required internal pressure. The pressure created in the heat pipe can be checked by manipulating the valves.
5. After attaining the required pressure, the valves towards the pump from the liquid filling will be closed and the distilled water filled.
6. All valves closed and the vice presses gently on heated point of the pipe for maximum joining process. Welding is done together with joining by vice for leakage not to occur
7. Testing for leakage. The heat pipe is checked for leakage by heating and registration the boiling temperature which corresponds the saturation pressure

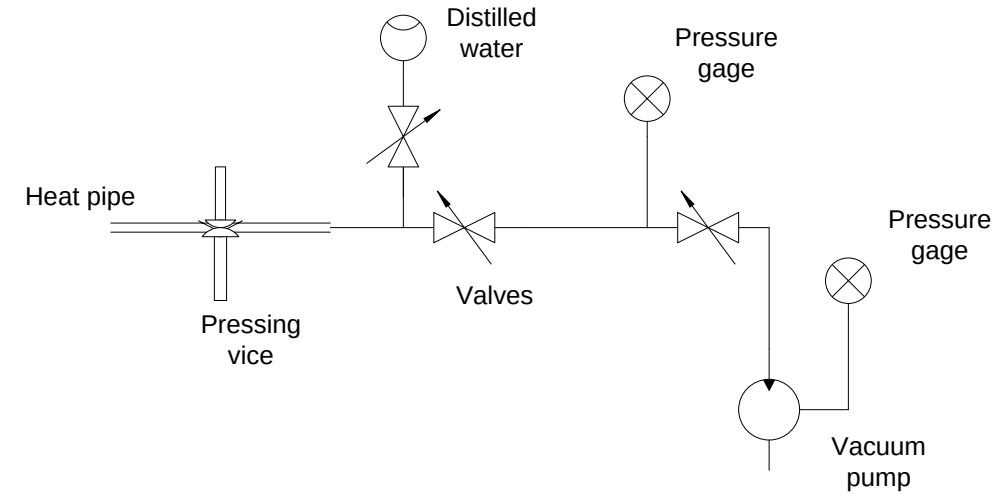

(a)

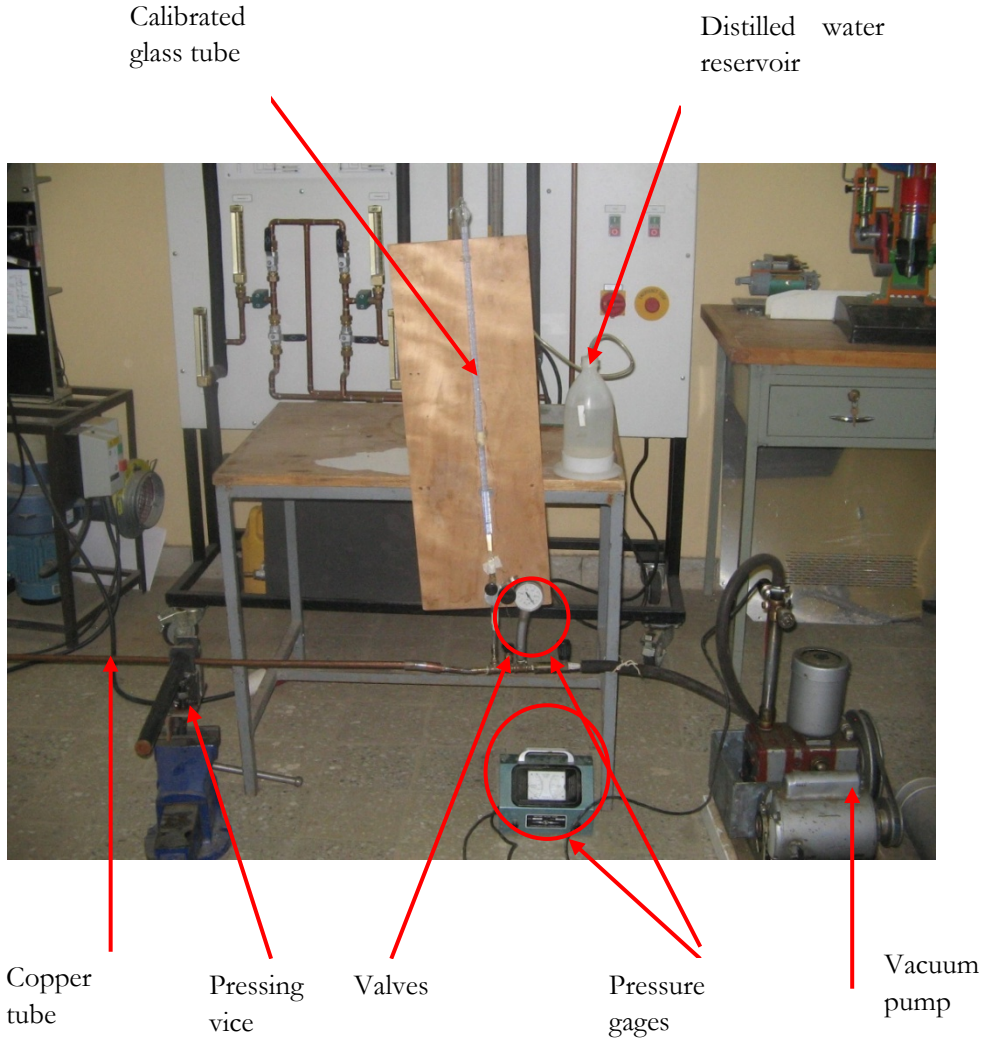

(b)

Figur 15. (a) Heat pipe manufacturing model (b) laboratory heat pipe manufacturing set up

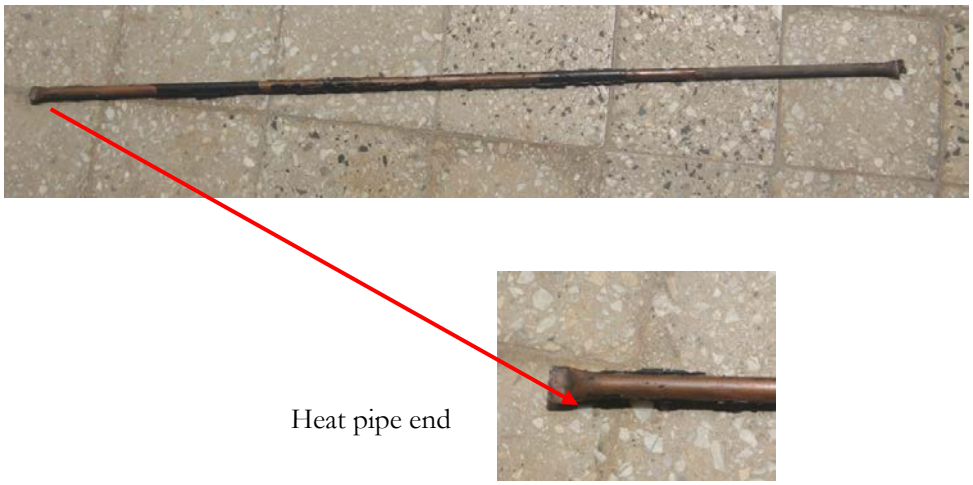

Figur 16. Manufactured heat pipe

Figur 17. Heat pipe testing set up

Table 1. Dimensions and properties of heat pipes manufactured

Property	Value	Property	Value
Liquid density ρ_l	988 kg/m3	Weak permeability K_p	1.24 x 10^{-9} m^2
Liquid viscosity μ_l	0.5588 x 10^{-3} Ns/m^2	Mesh wire diameter $d_{w,mesh}$	0.2 mm
Surface tension σ	0.0679 N/m	Heatpipe total length l_t	1.68 /1.08m
Vapor density ρ_v	0.08 kg/m3	Effective capillary radius r_e	2.5 x 10^{-4} m
Evaporator length l_{evap}	1.34 /0.7*	Gravitational acceleration g	9.81 m/s^2
Condenser length l_{cond}	0.3 m/0.34	Vapor specific heat ratio γ_v	1.32
Adiabatic length l_{adab}	0.04 m	Temperature of vaporization T_s	49 ^{0}C
Wick area A_w	1.9 x 10^{-5} m^2	Stagnant temperature T_0	49 ^{0}C
Gas constant R_v	461.5 J/kg .K	Latent heat of vaporization H	2382.8 KJ/kg
Internal pipe diameter $d_{i,hp}$	11 mm	Angel of inclination β	14 ^{o}
External pipe diameter $d_{0,hp}$	13 mm	Pipe material thermal conductivity k_{hp}	386 $W \cdot m^{-1} \cdot {}^0C^{-1}$
Vapor core diameter $d_{c,v}$	10.6 mm	Hydraulic radius of porous layer r_{hyd}	1.4 x10^{-5} m
Wick porosity ε	0.7	Heat pipe effective length l_{ef}	0.86 /0.553m
Equivalent thermal conductivity k_w	1.2 $W \cdot m^{-1} \cdot {}^0C^{-1}$	Filling Ratio	30%

*The yy/xx is the dimensions of two heat pipes for experiments (long/small heat pipes)

6.2. Manufacturing of Collector Systems

Two set of collectors have been manufactured based on the size of two successful heat pipes. One with forced convection system and the other without forced (natural circulation system). These two collectors are not identical in dimension but identical in construction materials. Figure 18 and 19 show collectors manufactured for performance testing. The pipe lines and water tanker are insulated by commercial cotton. Table 2 and 3 shows the dimensions and materials used during manufacturing.

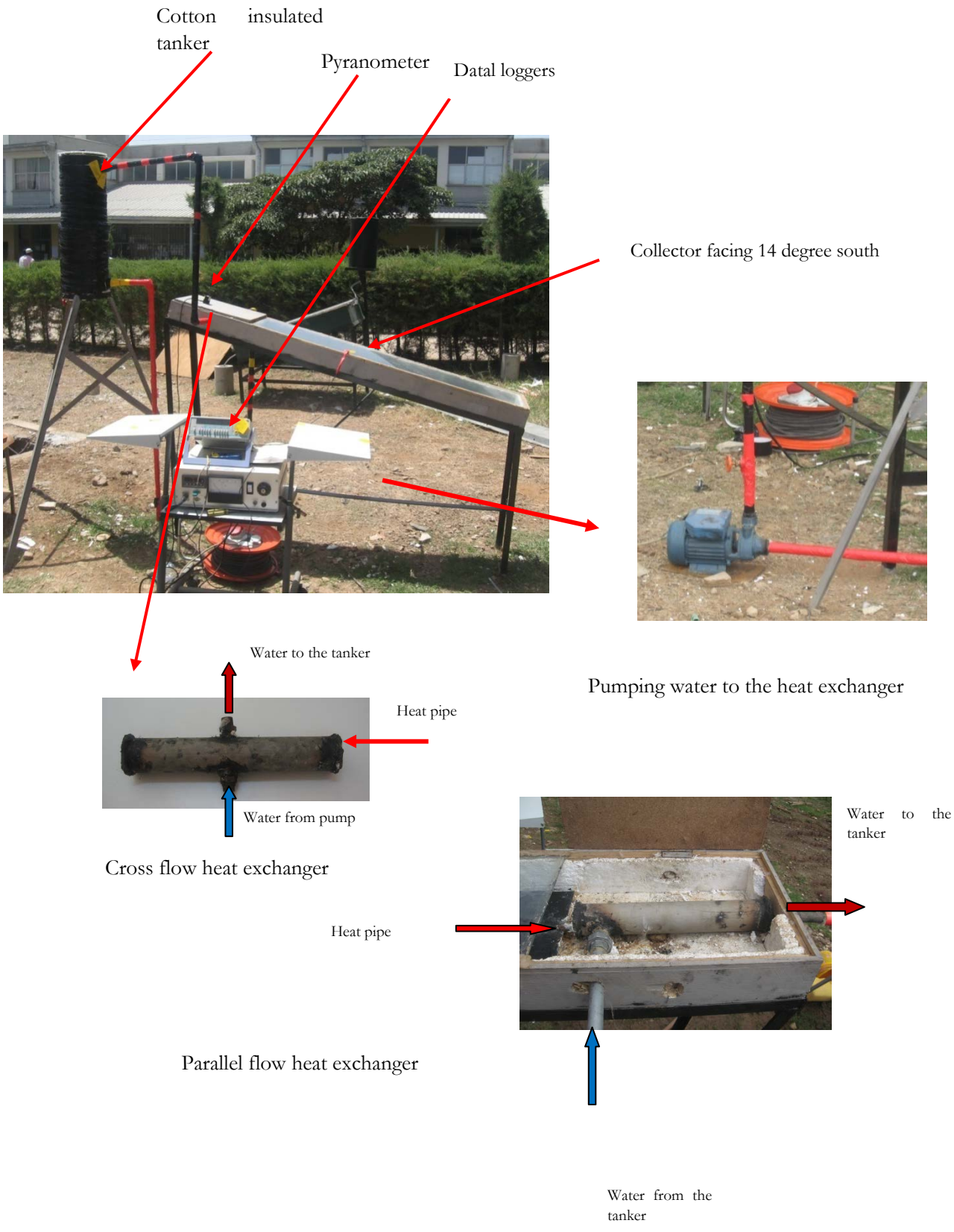

Figur 18. Manufactured prototype for forced convective heat pipe solar collector for solar water heater

Figure 19. Manufactured prototype for natural circulation and natural convective heat pipe solar heater

Figure 20. Heat pipe and absorber attachment

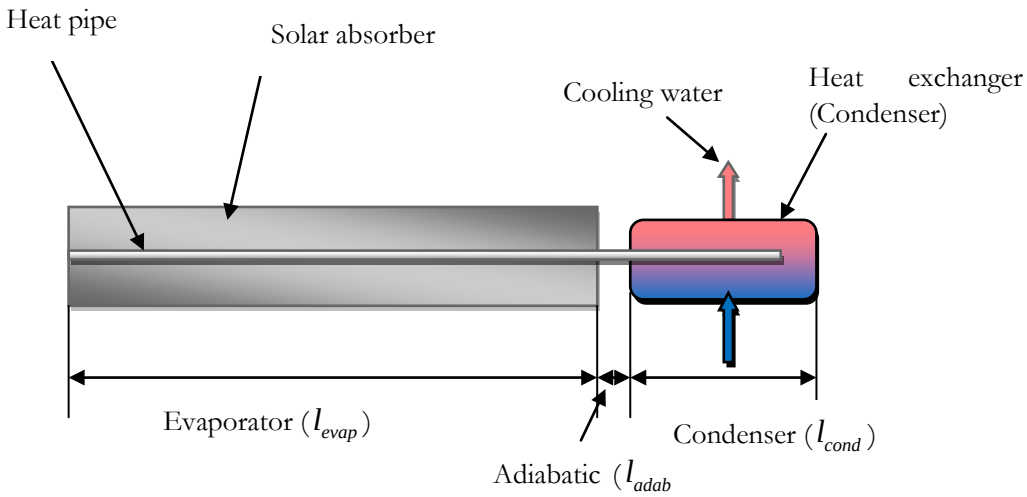

Figure 21. Configuration of heat pipe solar collector with forced convective condenser

Table 2. Heat pipe solar collector dimensions

Type of collector		Absorber Dimensions [mxm]	Storage Capacity [Liter]	Heat pipe condenser length [m]	Heat pipe Evaporator Length [m]	Heat pipe Condenser type	Test possibilities
Small collector	Heat pipe installation	0.24 x 0.7	5	0.34 m	0.7 m	Natural convective	Performance of heat pipe with natural convection condenser
	Natural circulation	0.24 x 0.7	5	-	-	-	Performance of natural circulation solar water heating
Forced heat pipe collector		0.24 x 1.34	35	0.3	1.34	Cross flow and parallel flow	Performance heat pipe with forced convective condensers of cross flow and parallel flow heat exchanger

Table 3. Material and their properties used in the manufacturing of solar collectors

Materials Used	Function	Density Kg/m^3	Thermal conductivity (W/m^{o}C)	Specific Heat capacity (kJ/kg^{o}C)	Dimension	Thickness	mCp (kJ/0C)	Remark
Aluminum sheet	Absorber	2707	204	0.996	0.24 x 1.34 m^2	0.8 mm	0.694	
		2707	204	0.996	0.24 x 0.7 m^2	0.8 mm	0.362	
Wood (pulp)	Collector Insulators and structure	600	0.17	0.42	8.5x0.1m^2	30mm	6.426	
		600	0.17	0.42	3.8x0.1m^2(small)	30 mm	2.873	
Foam	Insulation	40	0.036	1.3	0.4m^2	15mm	0.312	
		40	0.036	1.3	0.2 m^2	15mm	0.156	
Steel tube	Water circulation	7800	52	0.45	6mx ф0.021m	2.3mm	3.2	
Cotton	Insulation	ϱ	0.039	Cp	0.55 m^2	10 mm	0.0715	ϱ Cp=13KJ/m^{3}K
Copper	Heat pipe container	900	386	0.385	1.68 mx ø0.013m	~1 mm	0.24	
		900	386	0.385	0.77 mx ø0.013m	~1 mm	0.11	
Glass	Cover	2500	0.8	0.84	0.3 x 1.4 m^2	3.2 mm	2.8224	
		2500	0.8	0.84	0.3 x 0.8 m^2	3.2 mm	1.6128	
Steel sheet	For development of tankers	7800	52	0.45	0.72x0.72m2	1mm	1.82	D= 0.24 m
		7800	52	0.45	0.25x0.4 m2	1mm	0.351	
Copper wire	Joining	9000	386	0.385				

6.3. Measurement System

Measurement system design is one of the important tasks in experimental tests. In order to measure the performance of a collector basic parameters have to be measured. In collector system parameters that need good measurement system are: temperature, flow, and solar radiation. Water temperature in and out from the collector, ambient temperature to calculate heat loss from the system, and sometimes absorber and cover temperature are some of the variables which need temperature measurement system. Because of the limitation of availability of sensors in market, the measurement system has been designed from sensors which are designed for different purpose in Thermofluid laboratory. The system has been designed and calibrated to measure collector parameters.

Temperature measurement

Thermocouples and thermometers were used in measuring liquid, cover, absorber and ambient temperatures. K-type thermocouples were used to measure the temperature of the out and inlet water temperature of the collector heat exchanger. The ambient temperature has been measured using mercury thermometer. The whole measurement set up is shown in Figure 22. A digital display data logger was used for reading the temperature scale. The data logger was designed for other heat transfer measurement and had to be calibrated for this experiment and it was calibrated using number mercury thermometers as a reference.

Solar radiation measurement

A pyranomter with the following specification from Campbell Scientific model SP1110 was used to measure the global solar (both beam and diffuse) radiation. A digital voltmeter was used to read the signal out from the sensor. The measurement set is shown in Figure 22.

- Sensitive to light between 350nm and 1100nm
- Sensitivity :1mV per 1Wm^{-2}
- Cosine corrected head (typical errors: zero for 0-70°, <10% for 85-90°)
- Blue-enhanced silicon photocell detector with low fatigue characteristics
- Operating temperature : -35°C to +75°C
- Absolute accuracy: ±5% (typically <±3%)
- Standard cable: 3m

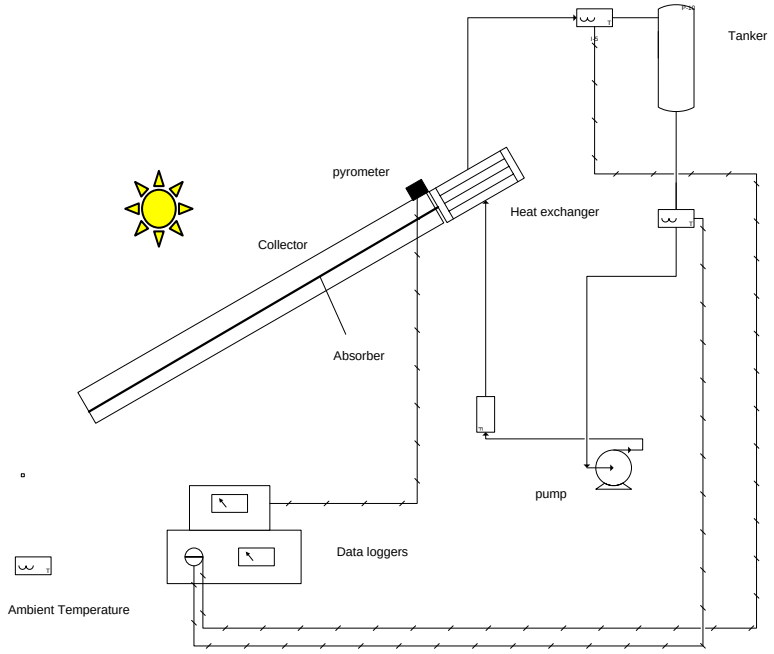

Figure 22. Measurement system design

Flow Measurement: a flow meter from FLOKAL® of model MT3809 is calibrated to measure the steady state flow from the pump to the collector. It is variable area flow meters are rugged, all metal flow meters offering 2% full scale accuracy. Flow rate indication is provided by means of magnetic coupling where a magnet, encapsulated in the float, is coupled to a rotatable magnet located in the rear of the indicator, thus turning the dial indicator mounted on the meter. At steady state pump speed, the fluid flow was found 25 liter/minute.

6.4. Experimental Testing Procedures

The experiment was designed to collect basic parameters to evaluate the performance of a collector. All collectors are faced towards south 14 degree inclination from the horizontal. The test was performed during the summer season of the year which has very cloudy days and it has been difficult to get clear day. Fortunately, this created an opportunity to test the system at low solar radiation level of the year.

Test for natural circulation and natural convective heat pipe solar collector: Because of low tanker volume, it was difficult to measure the inlet and outlet fluid temperature rather mean temperature of the tanker was measured. The data has been registered for each 30 minute time interval. Most experiments were started at 9:00 am of the morning. The global solar radiation and the ambient temperature were taken for each mean tanker temperature.

Test for forced convective heat pipe solar collector- Unlike the natural and heat pipe without forced system, it is important to measure and was possible to measure the inlet and outlet fluid temperatures

from the collector heat exchanger. The time interval is the same for both cases. The absorber and cover temperature measurement were taken using online thermocouple systems.

7. Result and Discussion

7.1. Heat Transfer Limits of Heat pipe

Based on the design dimensions of collectors and heat pipe, the critical design criteria is considered to check the limits of the heat pipe heat transport. The collector system is supposed to work in all conditions throughout the year and the maximum radiation level is considered as a critical value. A value of 1.1 kW/m^2 solar radiation is used for the design. A collector of the same length with evaporator and a width of 0.24 m designed for optimized fin efficiency. With this radiation level, the maximum heat that the heat pipe transfer is 0.354 kW. Table 4 shows a summary of the heat transfer limits for the heat pipe. The values obtained are well above the critical design value and the heat pipe is safe for operation. Capillary limit can be ignored for this specific due to the gravity assistance for the return of the condensate. However, the presence of wick capillarity in the heat pipe can enhance the uniform distribution of condensate in the evaporator to avoid the drawback of thermosyphon in solar collectors discussed in section 3.3.

Table 4. Heat pipe heat transfer limits

Type	Formula	Value
Sonic limit	$Q_{\max} = A_v \rho_v H \left[\frac{\gamma_v R_v T_v}{2(\gamma_v + 1)} \right]^{0.5}$	≈3.46 kW
Entrainment limit	$Q_{\max} = A_v H \left[\frac{\sigma_l \rho_v}{2 r_h} \right]^{0.5}$	≈0.45 kW
Boiling limit	$Q_{\max} = \frac{2\pi l_t k_e T_v}{H \rho_v \ln\left(\frac{r_i}{r_v}\right)} \left[\frac{2\sigma_1}{r_o} - P_o \right]$	≈1.62 kW

7.2. Natural Circulation Solar Water Heater

The thermal performance of natural circulation solar water heating was tested on June 27, 2008 at Mekelle University using the small solar collector setup with batch type water tank. Figure 23 shows the profile solar radiation measured on the test day. Due to summer season, it has been difficult to get a clear day to do performance test and several trials have been done to get good daily solar curve. This data was one of the best clear days for performance test.

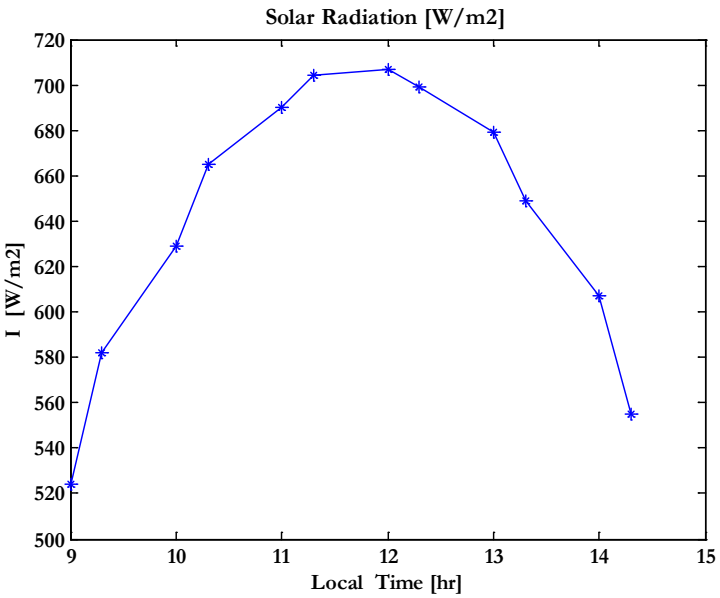

Figure 23. Solar radiation on June 27, 2008 at Mekelle University

The temperature increase in the water tanker is shown in Figure 24. As can be seen from the diagram the model and experimental data showed a good agreement. It was noticed that the maximum tanker temperature was 49.5 ^{o}C. After 14:00 hours, tanker temperature starts to decrease due to increase in heat loss and decrease in solar radiation. Due to decrease in solar radiation, the ambient temperature also starts to decrease. Higher tanker temperature increases the heat loss both in tanker and collector. High water temperature in the tanker increases the collector inlet temperature and increase the mean temperature of the collector which leads higher heat loss to ambient. Figure 25 shows the profile of theoretical collector mass flow rate as function of local time obtained by MATLAB. Collector mass flow rate showed similar trend with solar radiation profile. The mass flow rate is maximum value around noon when the solar radiation is maximum value. Decrease in solar radiation and the increase collector inlet temperature can cause to decrease the mass flow rate in absorber tube. When the temperature difference between inlet and outlet collector temperature is small value, the mass flow become small value, too.

Collector instantaneous efficiency was found to vary according to the external conditions i.e. solar radiation, ambient temperature and mean tanker temperature. This external conditions can be represented

by (Tw-Ts)/I and the collector instantaneous efficiency can be plotted against (Tw-Ts)/I as in Figure 27. The efficiency curve of experimental results agreed with model. The collector system showed higher efficiency at low tank temperature and the efficiency decreases as the tank temperature increases. Using curve fitting technique, linear equations are developed for both model and experiment curves to compare the sensitivity of efficiency with (Tw-Ta)/I. The equations are equivalent to

$$\eta = F_R \tau\alpha - F_R U_L \left(\frac{T_w - T_a}{I} \right)$$

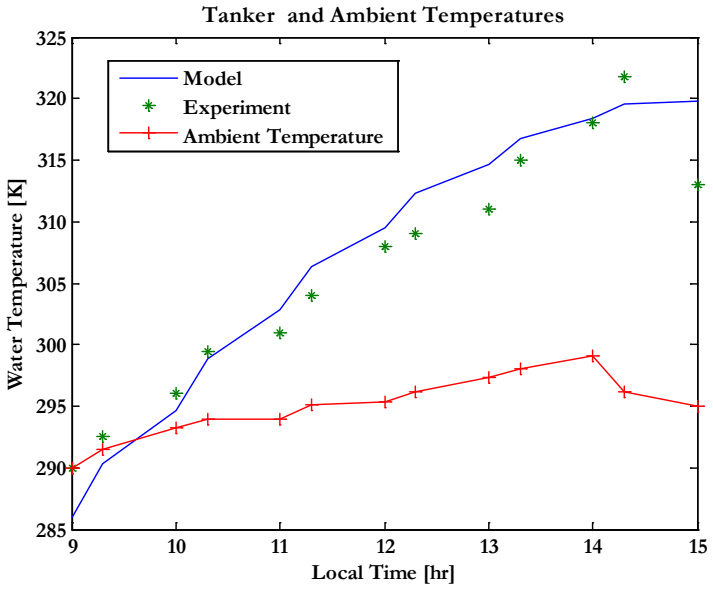

Figure 24. Temperature increase in water tank

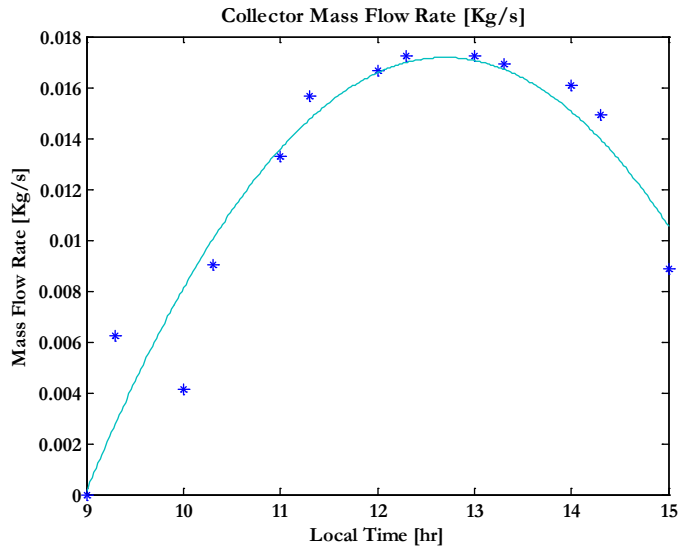

Figure 25. Collector mass flow rate during test hours

$F_R\tau\alpha$ is the y-intercept in the efficiency line and F_RU represents the slope of the curve. The higher the slope, the higher is the sensitivity to external conditions. Both experimental and model collector instantaneous curves have high slope value which indicates the efficiency is very sensitive to external condition. The heat transfer coefficient U_L also depends on the mean plate temperature. Khalifa (1999) experimentally investigated the impact of mean plate temperature on the total and collector top heat transfer coefficient. It was found the total and collector top heat transfer coefficient varies during the test

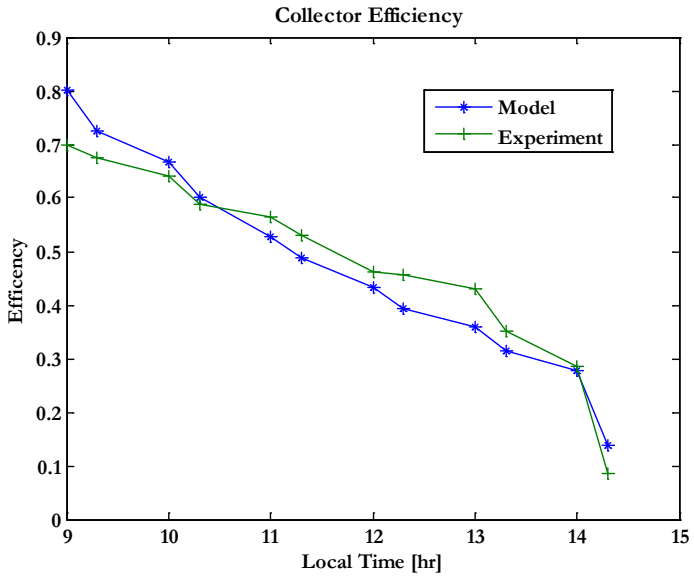

Figure 26 . Instantaneous efficiency during test hours

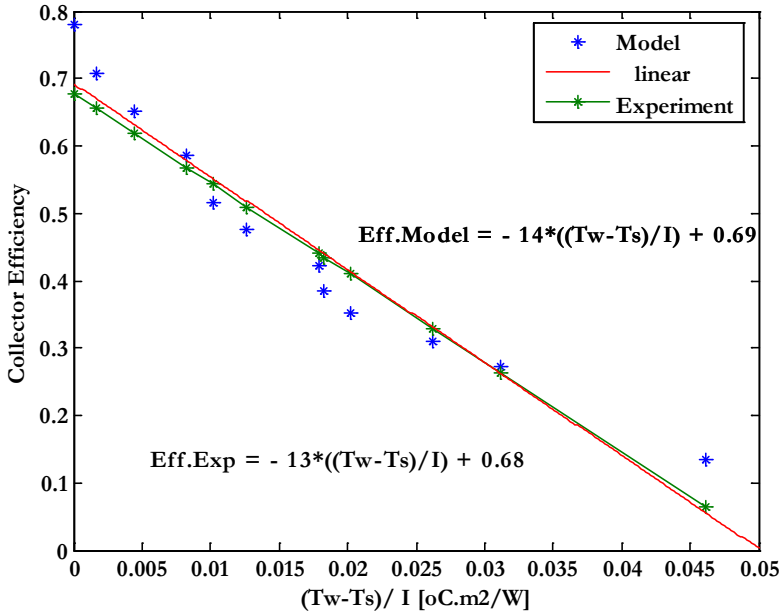

Figure 27. Collector instantaneous efficiency vs. (Tw-Ts)/I (Ts mean Ta)

hours due to the increase solar radiation and the mean absorber temperature. Higher collector inlet temperature increases the mean plate temperature and increases the collector total heat transfer coefficient which reduces the efficiency of the collector. Siddiqui (1997) has also studied a natural circulation solar water heater and found collector performance of lower than current study. The instantaneous efficiency was found between 20% to 50% while the y-intercept of 0.5 and slope of 6 was found in instantaneous efficiency vs. $(T_{fi}-T_s)/I$. The study showed a better slope compared to the current study because of the frequent withdrawal of hot water from the tanker and the collector inlet temperature T_{fi} is kept low for better performance of the collector. Figure 26 also supports the decrease of instantaneous efficiency during the collector test hours. Though the solar radiation increases up to noon, the efficiency kept to drop. This is due the increase of collector inlet temperature during test hours which is a common phenomenon for batch type of solar water heaters.

7.3. Heat Pipe Solar Collector with Natural Convective Condenser

Water rests on the hot condenser of the heat pipe and the water gets heated and rises up due to density difference. This phenomenon is natural convective heat transfer. Several researchers studied theoretically and experimentally wickless heat pipe (two-phase thermosyphon) and wicked heat pipe with natural convective condensing system for solar water heating. Mathioulakis and Belessiotis (2002) studied a two phase thermosyphon solar collector for water heating where the condenser section of the heat pipe was immersed in the tanker and a natural convective heat transfer was employed. Chun et al.(1999) studied heat pipe solar water heater in which the condenser is directly immersed to the storage tanker and the performance was compared with conventional natural circulation solar water heater. The main daily efficiency of heat pipe solar collector was found 7% higher than the conventional type (ca. 38%). Koffi et al. (2008) studied batch type two-phase thermosyphon solar water heater. The vapor produced in the thermosyphon system passes in coil heat exchanger in the tanker (internal heat exchanger) where natural convective heat transfer happens. The system has been validated both theoretically and experimentally and a mean collector efficiency of 58% was obtained. Mehmet Esen, and Hikmet Esen (2005) investigated the performance of two-phase thermosyphon using three different types of heat pipe working fluid: R-134a, R407C, and R410A where the condenser section of the heat pipe is directly passed inside the water tank and natural convective heat transfer happens. The maximum collection efficiencies of 50.84%, 49.43% and 48.72% for R410A, R407C and R-134a were found, respectively. The amount of latent heat for the refrigerants was found the limiting factor for heat transport.

The performance of natural convective heat pipe condenser has been tested on the same collector system as natural circulation type by replacing tubing systems. The test has been done on July 10, 2008 at Mekelle University and the solar radiation measured is shown in Figure 28. Figure 29 compares the numerical and experimental curves of water temperature as function of test hours and showed a good agreement. The

slight variation can be due to the dependency of heat transfer coefficient on temperature both in the condenser and in the collector system. After 13:30, the water temperature started to decrease. This can be caused by decrease in solar radiation and high tanker temperature which increases heat loss. Heat transfer in the condenser is favored by low water temperature. Figure 30 shows the instantaneous collector efficiency during the test hours. Collector efficiency of between 67% to 48% was obtained during the test hours. Figure 31 shows the effect of (Tw-Ts)/I on the efficiency of the collector.

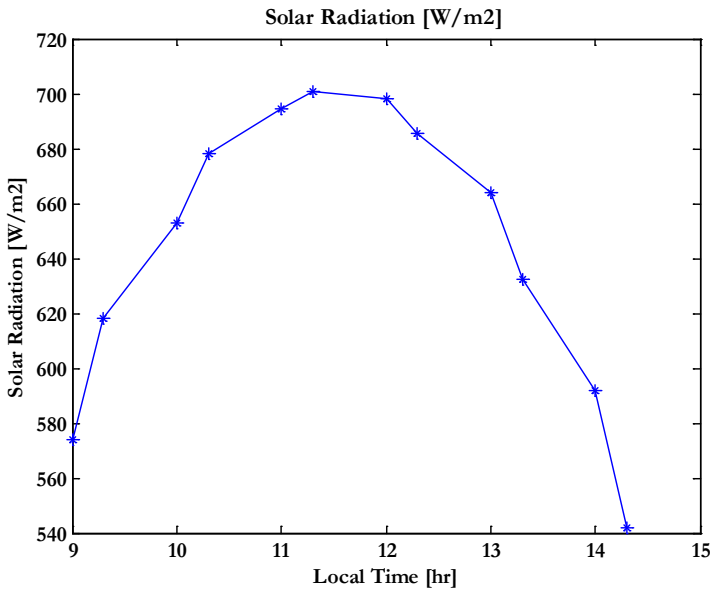

Figure 28. Solar radiation on July 10, 2008 at Mekelle University

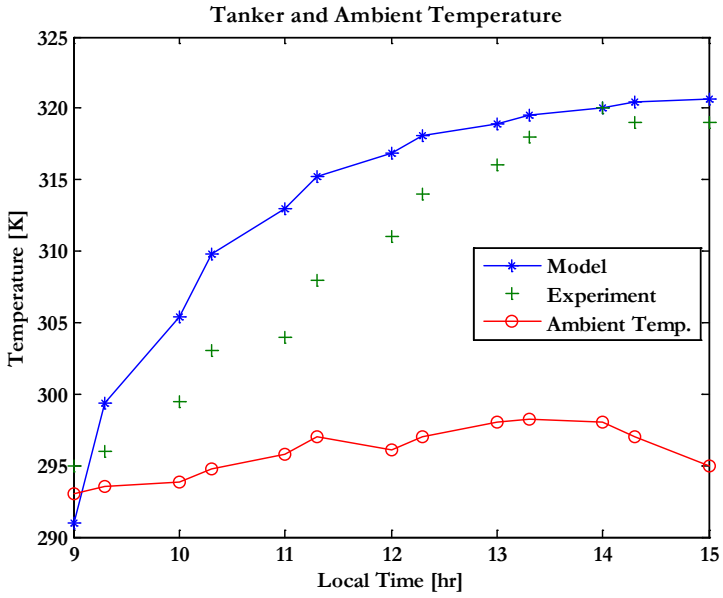

Figure 29. Water temperature increase during the test hours

Water as a working fluid for heat pipes have advantages compared with other refrigerants due to its high latent heat, nontoxic and compatible to most tube materials. Most thermosyphon solar collectors stated in

literatures are wickless and work by gravity. This led wickless heat pipes performance sensitive to design geometry. In wicked heat pipes such as heat pipes manufactured and used in this study, the sensitivity to geometry is less pronounced due to the capillary pressure developed inside the wick for uniform distribution of the condensate back to the evaporator section. In summary, based on results in Figure 30 and 31, this heat pipe solar collector showed one of the best performance compared with similar researches reported by Mathioulakis and Belessiotis (2002), Chun et al.(1999), Mehmet Esen, and Hikmet Esen (2005), Koffi et al. (2008), Chen et al. (2009), Huang et al.(2010).

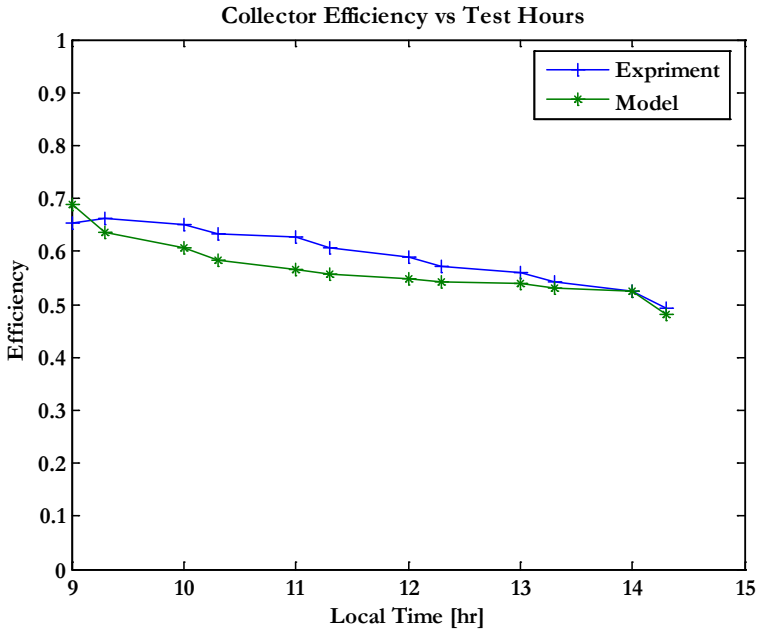

Figure 30. Instantaneous efficiency during test hours

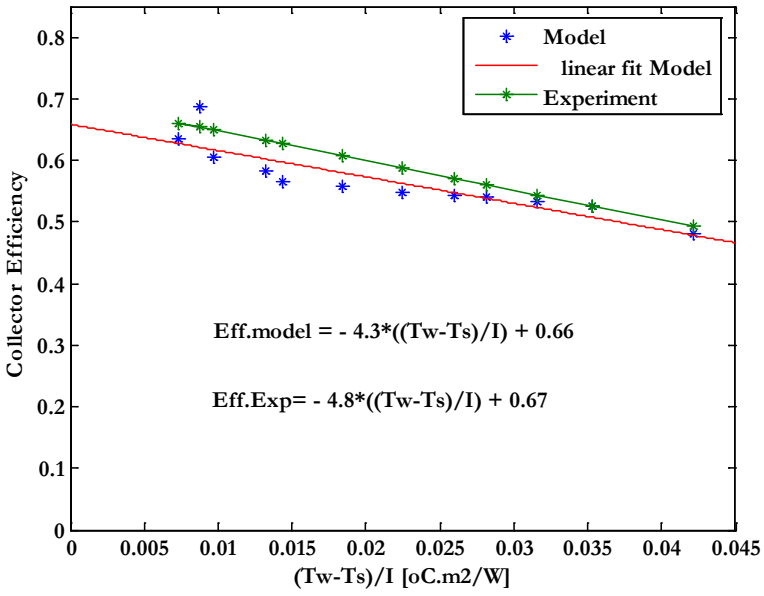

Figure 31. Collector instantaneous efficiency vs. (Tw-Ts)/I

7.4. Heat Pipe Solar Collector with Forced Convective Condenser

Forced convective is the most common type used in heat pipe condensers. Cooling water is pumped through heat exchanger where condensation of vapor takes place inside heat pipe condenser. These types of heat exchanger give a better heat transfer coefficient than natural convective types. A batch type of water heating using forced convective heat pipe solar collector was tested in this study. The heat exchanger can be designed as cross flow or parallel flow with condenser section. Both heat exchanger types have been tested and compared. Apart from the external conditions, performance of heat pipe solar collector with forced convective condenser depends on the working temperature of the heat pipe and water flow across heat exchanger. Wickless heat pipe solar collector with distilled water as working fluid was theoretically and experimentally investigated for water heating using cross flow heat exchanger for heat pipe condenser (Hussein, 2007). Optimum mass flow rate in the heat exchanger and number of heat pipe for best collector efficiency was found. A maximum instantaneous collector efficiency of 67% was found by experimental test at mass flow rate of close to ASHRAE standard. On the other side, as reported by Ismail and Abogderah (1998), higher mass flow rate in heat exchanger improved the heat transfer coefficient in the heat exchanger and improved the performance of heat pipe solar collector. Maximum efficiency has been obtained at mass flow rate of almost twice of the ASHRAE standard. Mass flows rate more than ASHRAE standard mass is also considered in this study for better heat transfer coefficient in the heat exchanger.

Tanker temperature increase as a function of test hours using cross flow heat exchanger is shown in Figure 32. The validation of experimental results by numerical modeling showed a good agreement. The numerical model showed a little higher compared with experimental results. This can be due to the heat transfer fouling and other unconsidered heat losses such as heat loss in the heat exchanger. The same phenomenon was seen in Figure 33 which shows the instantaneous collector efficiency. Similar to other collector tested, the performance is a function of external conditions. When comparing with literature reports, the collector showed an interesting performance. Similar performance was obtained compared to reports by Ismail and Abogderah (1998), Azad (2008), Riffat et al.(2005), Zhao et al.(2010) and Hussein, (2007).

The heat transfer coefficient in the condenser heat exchanger largely depends on the velocity of the cooling fluid, the cross sectional area and geometry of the flow channel. The two heat exchangers have been tested for the same flow but in different day. As can be seen from Figure 34 there is no significant difference in performance. This can be due to the high mass flow in the heat exchangers and turbulent flow in both cases which results high transfer coefficient. High heat transfer in the heat exchanger takes away the heat available efficiently and no significant difference was seen in the two heat pipe condensers.

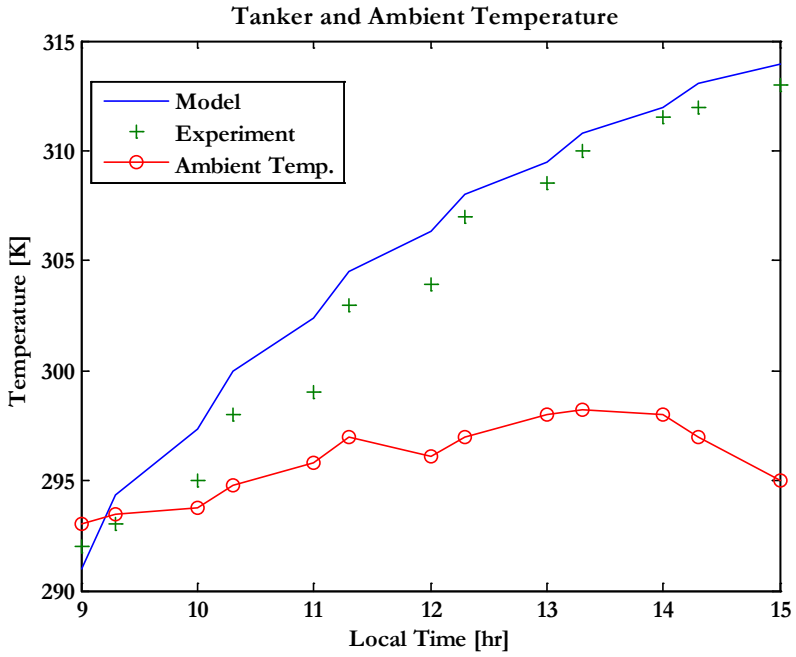

Figure 32. Water temperature increase in forced convective heat pipe solar collector- cross flow heat exchanger

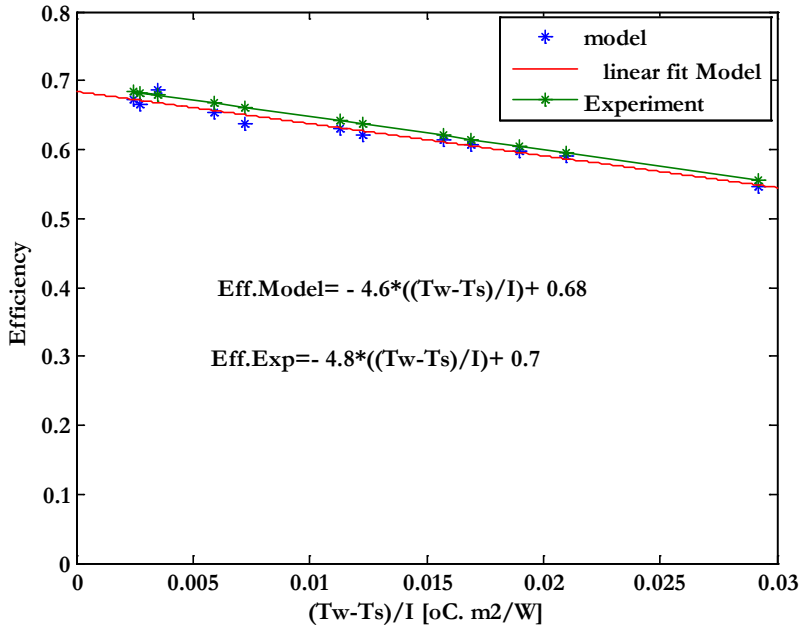

Figure 33. Collector instantaneous efficiency vs. (Tw-Ts)/I for heat pipe with forced convective condenser

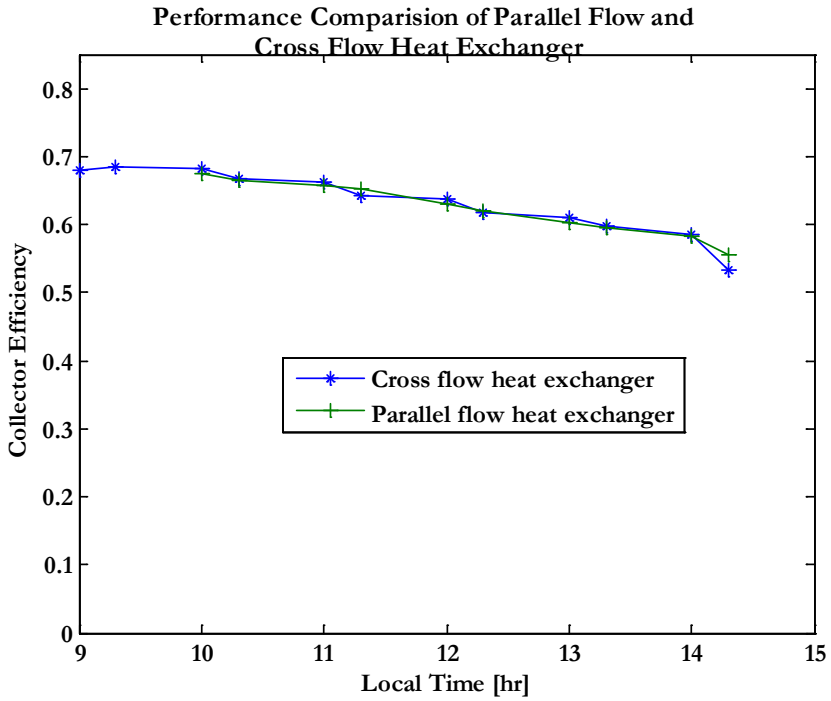

Figure 34. Efficiency comparison between parallel and cross flow heat exchanger for heat pipe condenser

7.5. Performance Comparison

Both numerical and experimental results have been analyzed for comparison purpose and found to have the same trend. Therefore, experimental results are presented for comparison purpose for simplicity. The performance of natural circulation solar water heater is greatly affected by external conditions. Figure 35 shows comparison instantaneous efficiency obtained by experimental data during test hours. Natural circulation solar water heater showed highest in the beginning and drastically decreased during the test hours compared to others. Low efficiency in the beginning is due to heat pipes start ups. Heat pipe start up is a complex phenomenon. To start up heat pipe operation, sufficient amount of heat flux has to be supplied to the evaporator (Reay and Kew, 2006). The low efficiency in the morning for heat pipe solar collector is due to low solar radiation in the morning which is not enough to meet minimum condition to start the heat pipe operation. The same phenomenon is reported by Ismail and Abogderah (1998). However, the heat pipe solar collectors have showed interesting performance without significant decrease of instantaneous efficiency as compared with natural circulation. As it was expected, the performance of forced heat pipe condenser was the highest due to its high heat transfer coefficient. Other similar studies reported similar phenomena when comparing heat pipe with conventional systems. Ismail and Abogderah (1998) have also reported on their report similar phenomenon when comparing the performance of methanol working fluid heat pipe solar collector with conventional natural circulation solar collector for water heating.

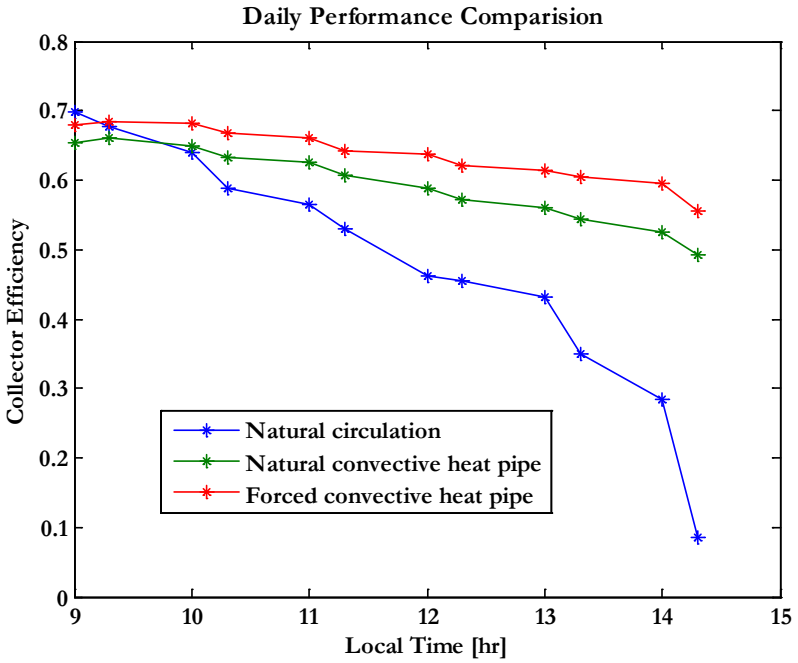

Figure 35. Comparison of instantaneous efficiency during test hours

Table 5 shows the comparison of experimental results. The y-intercept and slope of instantaneous efficiency is used to compare the performance of solar collectors. The intercept and slope of collector systems are obtained using best curve fitting technique in Matlab. The slope of natural circulation system is much higher compared with other types. This has made the collector very sensitive to external conditions. The heat loss is very sensitive to the water temperature. The slope of natural and forced convective heat pipe condensers was found to be the same value. This shows that tested heat pipe collectors is less responsive to external conditions. Figure 36 shows the instantaneous efficiency vs. (Tw-Ts)/I and the diagram supports what is discussed in Table 5. The heat transfer per area of collector is shown in Figure 37. The maximum heat transfer rate occurs between 10:00 to 11.30 hours of the day.

Table 5. Comparison of fitted curves of instantaneous efficiencies

Collector type	$F_R(\tau\alpha)$	F_RU_l
Conventional Natural Circulation	0.7	13
Natural convective condenser heat pipe	0.67	4.8
Forced convective condenser heat pipe with cross flow heat exchanger	0.7	4.8

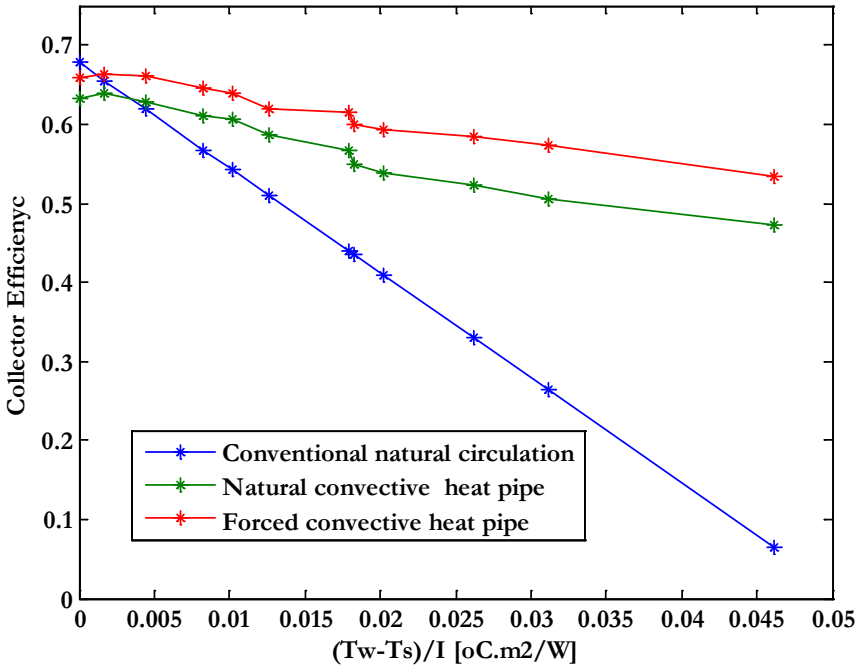

Figure 36. Comparison of Collector instantaneous efficiency vs. (Tw-Ts)/I

The performance of forced convective heat pipe solar collector has been found the most efficient among the studied collectors. However, this collector system requires a parasitic electrical power for pumping of fluids and works in the availability of electricity. In contrast to this, both natural convective heat pipe and natural circulation solar collector can work in the absence of electricity. The absence of parasitic electrical power makes them suitable technologies for rural communities of developing countries where electricity is scarce. These collector systems are also simpler in design and complexity compared to heat pipe solar collectors with forced convective condensers where substantial tubing and pumping systems are required. The main drawback of natural circulation water heater is its low efficiency compared to others and the requirement of operating tanker height from the collector. Besides the requirement of piping, it reduces aesthetic values of buildings when they are part of built environment. On the other side, heat pipe collector with natural convective condenser has showed substantial improvement in efficiency and simplicity. However, special design of tanker geometry is required so as to attain the maximum working efficiency. The designed geometries should facilitate maximum natural convective heat transfer coefficient.

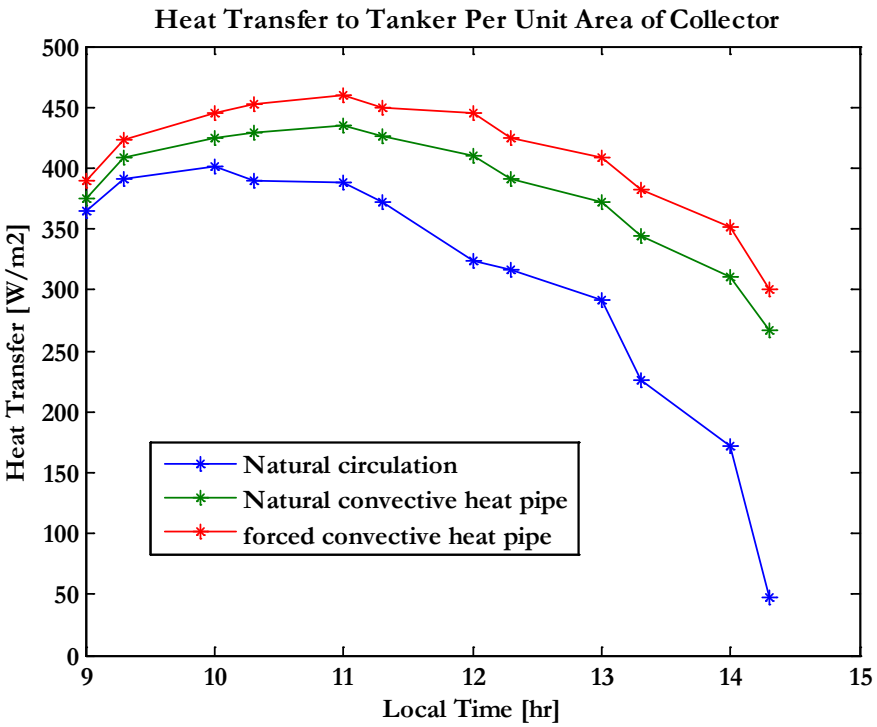

Figure 37. Comparison of heat transfer per unit area of collector systems

8. Conclusion

Efficiency of solar collector for water heating can be improved by designing appropriate design of heat transport system from solar absorber to heat storage system. The performance of heat pipe solar collectors was investigated both theoretically and experimentally under different heat pipe condenser types and compared with conventional natural circulation solar collector. Numerical and experimental results were found with good agreement. In both cases, heat pipe solar collectors outperformed compared with conventional natural circulation solar collector after start up. The obtained efficiency curve is very remarkable compared to related works mentioned in literatures. The performance of heat pipe collectors were found less sensitive to external conditions such as solar radiation , ambient temperature and tanker temperature. Due to steady state operation of heat pipes and better heat transport system from the absorber to the storage tank, the heat loss from collector due to tanker temperature increase was greatly reduced which increased system efficiency compared to conventional solar collectors.

Unlike conventional solar collectors, heat pipe solar collectors require a special design of heat exchanger for heat pipe condensers. Both natural and forced convective types of heat pipe condenser were tested in this study. Both cross flow and parallel flow forced convective heat pipe condensers were tested and no appreciable difference was noticed due to high mass flow in the heat exchanger which give higher heat transfer coefficient enough to take away all the available heat from the condenser. Forced convective heat

exchangers were found to have a better heat transfer coefficient compared with natural convective heat exchanger. However, appreciable performance was obtained for natural convective heat pipe condenser. The advantage of natural convective heat pipe condenser is that no parasitic power is required to run the system which makes the system suitable for rural communities where grid electricity is scarce. Moreover, natural convective heat pipe condensing system requires less tubing which makes them low cost compared with forced heat pipe solar collectors.

The performance of natural convective heat pipe condenser can be affected on the geometries of the condensers and further studies on the impact of natural condenser design geometries are required for better heat transfer coefficients. Moreover, further studied on the impact of collector parameters such as heat exchanger mass flow rate, different heat pipe bonding mechanisms with absorber and ratio of heat pipe evaporator to condenser section are required.

9. Reference

Aguilar C., White D.J., Ryan D. L., 2005, *Domestic water heating and water heater energy consumption in Canada. Canadian Building Energy End-use Data and Analysis Center*, CBEEDAC 2005–RP-02

Azad E., 2008, *Theoretical and experimental investigation of heat pipe solar collector*. Experimental Thermal and Fluid Science, 32 :1666–1672.

Chen B-R., Chang Y-W., Lee W-S., Chen S-L.,2010, *Long-term thermal performance of a two-phase thermosyphon solar water heater*. Solar Energy, 83: 1048–1055.

Chien C.C., Kung C.K., Chang C.C., Lee W.S., Jwo C.S., Chen S.L., 2011, *Theoretical and experimental investigations of a two-phase thermosyphon solar water heater*. Energy, 36: 415-423.

Close D. J., 1962, *The performance of solar water heaters with natural circulation*. Solar Energy,6:30–40.

Coulson J. M., Richardson J. F., Marker J. H., Backhurst J. R., 1999, *Coulson & Richardson's Chemical Engineering*, Volume 1, Sixth edition Fluid Flow, Heat Transfer and Mass Transfer, Butterworth – Heinemann Publishing, Oxford, UK

Duffie J A,. Beckman W. A, 1991, *Solar Engineering of Thermal Processes*, Second Edition, A Willy-Interscience Publication , USA.

Dunn P.D,. Reay D.A., 1994, *Heat Pipes*, Fourth Edition , Elsevier Science Ltd.

Energy in Sweden 2010, Swedish Energy Agency, online available http://webbshop.cm.se/System/TemplateView.aspx?p=Energimyndigheten&view=default&cat=/Broschyrer&id=b4cea7b00212456b9bdbdbe47a009474, May 2011.

Esen M., Esen H., 2005, *Experimental investigation of a two-phase closed thermosyphon solar water heater*. Solar Energy, 79 :459–468.

Faca˜o J., Oliveira A. C., 2005, *The effect of condenser heat transfer on the energy performance of a plate heat pipe solar collector*. International Journal of Energy Research, 29:903–912.

Faghri A., 1995, *Heat pipe science and technology*, Taylor and Francis publisher , Washington USA

Francis de Winter, 1990, *Solar Collectors, Energy Storage, and Materials*, Massachusetts Institute of Technology, USA.

Gupta C. L., Gargi H. P.,1968, *System design in solar water heaters with natural circulation*. Solar Energy,. 12: 163-182.

Hollands K.G.T.,Unny T.E.,Raithby G.D., Lonicek L., 1976, *Free convection heat transfer across inclined air layers*. Transaction of ASME journal of heat transfer, 98: 189-197.

Huang B. J., 1980, *Similarity theory of solar water heater with natural circulation*, Solar Energy, 25: 105-116.

Huang J., Pu S., Gao W., Que Y., 2010, *Experimental investigation on thermal performance of thermosyphon flat-plate solar water heater with a mantle heat exchanger*. Energy, 35:3563-3568.

Hussein H.M.S., 2007, *Theoretical and experimental investigation of wickless heat pipes flat plate solar collector with cross flow heat exchanger*. Energy Conversion and Management, 48:1266–1272.

Hussein H.M.S., Mohamad M.A., El-Asfouri A.S.,1999, *Optimization of a wickless heat pipe flat plate solar collector*. Energy Conversion & Management, 40:1949-1961.

Ismail K.A.R, Abogderah M. M., 1998, *Performance of a heat pipe solar collector*, Transaction of ASME, 120: 51-59.

Khalifa, A-J. N., 1999, *Thermal performance of locally made flat plate solar collectors used as part of a domestic hot water system*. Energy Conversion & Management, 40:1825-1833.

Koffi P.M.E., Andoh H.Y., Gbaha P., Toure S., Ado G., 2008, *Theoretical and experimental study of solar water heater with internal exchanger using thermosiphon system*, Energy Conversion and Management, 49: 2279–2290.

Kreider F.J. ,Kreith F., 1977, *Solar Heating and cooling: engineering, practical Design, and Economics*, Washington DC: Hemisphere Publishing Corporation, USA.

Mathioulakis E. and Belessiotis V., 2002, *A new heat-pipe type solar domestic hot water system*. Solar Energy, 72: 13–20.

Ong K. S., 1974, *A finite-difference method to evaluate the thermal performance of a solar water heater*. Solar Energy, 16 :137-147.

Payakaruk, T., Terdtoon, P., Ritthidech, S., 2000, *Correlations to predict heat transfer characteristics of an inclined closed two-phase thermosyphon at normal operating conditions*. Applied Thermal Engineering, 20:781–790.

Perry R.H., Green D.W.,1999, *Perry's chemical engineers handbook*, 7th Edition , McGraw-Hill Companies, Inc., USA

Reay D.A., Kew P.A., 2006, *Heat Pipes,* 5th Edition, Butterworth-Heinemann publisher, Oxford, UK.

Riffat S.B., Zhao X., Doherty P.S., 2005, *Developing a theoretical model to investigate thermal performance of a thin membrane heat-pipe solar collector*. Applied Thermal Engineering, 25: 899–915.

Siddiqui M. A., 1997, *Heat transfer and fluid flow studies in the collector tubes of a closed-loop natural circulation solar water heater*, Energy Conversion and Management,38:799-812.

Sodha M. S., Tiwari G. N.,1981, *Analysis of natural circulation solar water heating systems*. Energy Conversion and Management, 21: 283- 288.

Taherian H., Rezania A., Sadeghi S., Ganji D.D.,2011, *Experimental validation of dynamic simulation of the flat plate collector in a closed thermosyphon solar water heater*. Energy Conversion and Management, 52: 301–307.

Tardy F., Sami S. M., 2009, *Thermal analysis of heat pipes during thermal storage*. Applied Thermal Engineering, 29: 329–333.

US household electricity consumption report in 2001, released date July 2005 and available at http://www.eia.doe.gov/emeu/reps/enduse/er01_us_figs.html, May 2011.

Zerrouki A., Boume´dien A., Bouhadef K., 2002, *The natural circulation solar water heater model with linear temperature distribution*. Renewable Energy, 26: 549–559.

Zhao X., Wang Z. , Tang Q., 2010, *Theoretical investigation of the performance of a novel loop heat pipe solar water heating system for use in Beijing, China*. Applied Thermal Engineering, 30:2526-2536.